THE FASEB JOURNAL • RESEARCH • www.fasebj.org

# Low availability of choline *in utero* disrupts development and function of the retina

**Isis Trujillo-Gonzalez,* Walter B. Friday,* Carolyn A. Munson,* Amelia Bachleda,[†,1] Ellen R. Weiss,[†] Nazia M. Alam,[‡,§] Wei Sha,[¶] Steven H. Zeisel,[*,‖,2] and Natalia Surzenko[*,‖,3]**

[*]Nutrition Research Institute, University of North Carolina–Chapel Hill, Kannapolis, North Carolina, USA; [†]Department of Cell Biology and Physiology and [‖]Department of Nutrition, Gillings School of Global Public Health, University of North Carolina–Chapel Hill, Chapel Hill, North Carolina, USA; [‡]Department of Physiology and Biophysics, Weill Cornell Medical College, New York, New York, USA; [§]Center for Visual Restoration, Burke Neurological Institute, White Plains, New York, USA; and [¶]Bioinformatics Services Division, University of North Carolina–Charlotte, Kannapolis, North Carolina, USA

**ABSTRACT: Adequate supply of choline, an essential nutrient, is necessary to support proper brain development. Whether prenatal choline availability plays a role in development of the visual system is currently unknown. In this study, we addressed the role of *in utero* choline supply for the development and later function of the retina in a mouse model. We lowered choline availability in the maternal diet during pregnancy and assessed proliferative and differentiation properties of retinal progenitor cells (RPCs) in the developing prenatal retina, as well as visual function in adult offspring. We report that low choline availability during retinogenesis leads to persistent retinal cytoarchitectural defects, ranging from focal lesions with displacement of retinal neurons into subretinal space to severe hypocellularity and ultrastructural defects in photoreceptor organization. We further show that low choline availability impairs timely differentiation of retinal neuronal cells, such that the densities of early-born retinal ganglion cells, amacrine and horizontal cells, as well as cone photoreceptor precursors, are reduced in low choline embryonic d 17.5 retinas. Maintenance of higher proportions of RPCs that fail to exit the cell cycle underlies aberrant neuronal differentiation in low choline embryos. Increased RPC cell cycle length, and associated reduction in neurofibromin 2/Merlin protein, an upstream regulator of the Hippo signaling pathway, at least in part, explain aberrant neurogenesis in low choline retinas. Furthermore, we find that animals exposed to low choline diet *in utero* exhibit a significant degree of intraindividual variation in vision, characterized by marked functional discrepancy between the 2 eyes in individual animals. Together, our findings demonstrate, for the first time, that choline availability plays an essential role in the regulation of temporal progression of retinogenesis and provide evidence for the importance of adequate supply of choline for proper development of the visual system.—Trujillo-Gonzalez, I., Friday, W. B., Munson, C. A., Bachleda, A., Weiss, E. R., Alam, N. M., Sha, W., Zeisel, S. H., Surzenko, N. Low availability of choline *in utero* disrupts development and function of the retina. FASEB J. 33, 9194–9209 (2019). www.fasebj.org**

**KEY WORDS: retinal development · Nf2/Merlin · visual sensitivity · maternal nutrition**

Choline is an essential nutrient and is vital for multiple cellular functions (1). Choline is a precursor for acetylcholine, a neurotransmitter, as well as for phosphatidylcholine, a major constituent of cellular membranes (2, 3). Importantly, choline is also a methyl group donor. *S*-adenosylmethionine is produced through the choline metabolism pathway, among others, and is an essential substrate in DNA, RNA, and protein methylation reactions (4). Through its multiple roles, including regulation of gene and protein expression *via* DNA and histone

**ABBREVIATIONS:** BrdU, bromodeoxyuridine; c/d, cycles per degree; CFP, cyan fluorescent protein; E, embryonic day; EdU, 5-ethynyl-2′-deoxyuridine; EGFR, epidermal growth factor receptor; ERG, electroretinography; GCL, ganglion cell layer; IdU, iododeoxyuridine; Islet1, ISL LIM Homeobox 1; NBL, neuroblastic cell layer; Nf2, neurofibromin 2; NPC, neural progenitor cells; Olig2, oligodendrocyte transcription factor 2; OLM, outer limiting membrane; ONL, outer nuclear layer; P, postnatal day; PAK1, p21-activated kinase 1; PH3, phosphohistone 3; PNA, peanut agglutinin; RGC, retinal ganglion cell; RPC, retinal progentitor cell; Sall3, spalt-like transcription factor 3; sf, spatial frequency; TAZ, tafazzin; TM, tamoxifen; YAP, Yes-associated protein

[1] Current affiliation: Institute for Learning and Brain Sciences, University of Washington, Seattle, WA, USA.
[2] Correspondence: Nutrition Research Institute, University of North Carolina–Chapel Hill, 500 Laureate Way, Room 2218, Kannapolis, NC 28081, USA. E-mail: steven_zeisel@unc.edu
[3] Correspondence: Nutrition Research Institute, University of North Carolina–Chapel Hill, 500 Laureate Way, Room 2204, Kannapolis, NC 28081, USA. E-mail: surzenko@email.unc.edu

doi: 10.1096/fj.201900444R
This article includes supplemental data. Please visit *http://www.fasebj.org* to obtain this information.

 0892-6638/19/0033-9194 © FASEB

methylation, choline availability serves to modulate tissue growth and homeostasis (1).

Dietary intake of choline in humans varies greatly, with only 7% of women in the developed countries, and even fewer in the developing countries, achieving the recommended levels of choline intake (1, 5–9). In addition, single nucleotide polymorphisms affecting choline metabolism genes, such as phosphatidyl-*N*-methyltransferase, are prevalent among women (10, 11). Together with insufficient dietary intake, single nucleotide polymorphisms in choline metabolism genes may lead to less than adequate supply of choline to the developing fetus during pregnancy, possibly affecting the critical early steps of CNS development and consequently later cognitive function.

In the developing rodent brain, adequate choline availability is necessary for the maintenance of a sufficient pool of neural progenitor cells (NPCs) to sustain neurogenesis (12–14). When choline levels in the maternal diet are low, NPC self-renewal capacity in the fetal brain is compromised, leading to precocious NPC differentiation. In the developing mouse cerebral cortex, low availability of choline between d 11 and 17 of gestation manifests in the reduction in cortical NPCs, radial glia, and intermediate progenitor cells specifically (12). Consistent with premature differentiation and depletion of cortical NPCs due to low choline availability, production of the early born, lower layer (layer VI) cortical neurons is increased, whereas genesis of the later born, upper layer neurons (layers II–IV) is reduced in low choline embryonic brains. Conversely, if maternal dietary intake of choline in rodents during pregnancy is increased above adequate, the offspring perform better on spatial and visual memory tests throughout life (15–18). In humans, a significant enhancement in an infant's information processing speed at 4–13 mo of age was observed in children whose mothers were supplemented with choline chloride (930 mg/d of choline equivalents *vs.* 480 mg/d during pregnancy) (19), whereas higher dietary choline intake in pregnant mothers was associated with better cognitive performance in their children at 7 yr of age (5). Yet, the long-term consequences of low supply of choline for the development of the visual system are unknown.

Developing retina is a sensitive model system, which can be used to study the impact of environmental factors, such as dietary nutrients, on neurogenesis. Retina is derived from the neuroepithelium of the ventral diencephalon and thus shares its origin with the rest of the brain (20). The temporal progression of retinal neuronal cell differentiation is well understood and is conserved among vertebrates (21, 22). In the mouse, retinogenesis begins at embryonic day (E) 11.5 and continues through postnatal day (P) 10. Retinal ganglion cells (RGCs) are the first neurons that begin differentiation in the retina, followed by cone photoreceptors, horizontal cells, and amacrine cells, the majority of which are born during embryonic stages of mouse retinal development. Rod photoreceptors, bipolar cells, and Müller glia, on the other hand, are born predominantly postnatally. Importantly, retinal progenitor cell (RPC) proliferative and differentiation properties rely on precise temporal regulation of key signaling pathways and transcription factors that control RPC fate, but they can also be influenced by environmental factors (23, 24).

In this study, we addressed the role of choline supply in prenatal mouse retinal development. We hypothesized that similarly to the developing cerebral cortex (12), choline availability may be required to regulate proliferative and differentiation properties of RPCs in the developing retina. We found that low availability of choline during prenatal mouse retinogenesis inhibits RPC cell cycle exit and neuronal differentiation, leading to long-lasting changes in retinal cytoarchitecture and function. Thus, our data suggest that adequate availability of dietary choline to the embryo is essential for proper development and later function of the visual system.

## MATERIALS AND METHODS

### Animals

Animal experiments were performed in accordance with the protocols approved by David H. Murdock Research Institute Institutional Animal Care and Use Committee. *NestinCFPnuc* animals were a gift from Dr. Enikolopov (Renaissance School of Medicine, Stony Brook University, Stony Brook, NY, USA) (25). *Nestin-CreER$^{T2}$* (stock number: 016261) (26), *Ai9* (stock number: 007909) (27) and C57BL/6J (stock number: 000664) mouse lines were obtained from The Jackson Laboratory (Bar Harbor, ME, USA); *NestinCFPnuc*, *Nestin-CreER$^{T2}$*, and *Ai9* lines were maintained on C57BL/6J background. Genotyping was performed according to published protocols (25–27) and those used at The Jackson Laboratory. Genotyping of *NestinCFPnuc* animals was performed using the following primers detecting cyan fluorescent protein (CFP): NestinCFPnuc F 5′-ATCACATGGTCCTGCTGGAGTTC-3′, NestinCFPnuc R 5′-GGAGCTGCACACAACCCATTGCC-3′. Genotyping of *Nestin-CreER$^{T2}$* animals was performed using the following set of primers: NestinCre F 5′-GCGGTCTGGCAGTAAAAACTATC-3′; NestinCre R 5′-GTGAAACAGCATTGCTGTCACTT-3′; Positive control F 5′-CTAGGCCACAGAATTGAAAGATCT-3′; Positive control R 5′-GTAGGTGGAAATTCTAGCATCATCC-3′. Genotyping of *Ai9* animals was performed using the following set of primers for *Rosa26* locus and the knock-in reporter allele: Ai9WT-F 5′-AAGGGAGCTGCAGTGGAGTA-3′; Ai9WT-R 5′-CCGAAAATCTGTGGGAAGTC-3′; Ai9KI-F 5′-GGCATTAAAGCAGCGTATCC-3′; Ai9KI-R 5′-CTGTTCCTGTACGGCATG G-3′. Timed mating was used to generate litters for analyses, and day of plug detection was considered d 0.5 of gestation.

### Diets

Experimental animals were acclimated to defined diets at least 1 wk prior to mating and maintained on defined diets throughout experiments. Pregnant dams (multiple batches of 3–5 dams per group) were randomly assigned to either adequate or low choline group; low choline diet was administered starting at d 11.5 of pregnancy. Main reported findings (retinal structural dysgenesis, retinogenesis defects, and cone photoreceptor ultrastructure) were studied in animals raised on a modified AIN93G diet (M-AIN93G) (D16040706N and D16040705; Research Diets, New Brunswick, NJ, USA; and 103186 and 103187; Dyets, Bethlehem, PA, USA), and on AIN76A diet (110098 and 118853; Dyets). Structural dysgenesis results were also confirmed in animals raised on Open Source defined chow diet (D11112201 and D13090101-02; Research Diets) (also see Supplemental Table S1).

Low choline diet contained 0 g/kg diet of choline chloride (AIN93G and AIN76A) or choline bitartrate (Open Source defined chow). Adequate choline diet contained 1.4 g/kg of choline chloride (M-AIN93G), 1.2 g/kg of choline chloride (AIN76A), and 2 g/kg of choline bitartrate (Open Source defined chow). Animals raised on chow 6F 5K52 (The Jackson Laboratory) were used to establish conditions for spatial visual function measurements.

### Electroretinography

C57BL/6J mice, ranging in age from P35 to 4 mo, which were exposed to adequate or low choline diets during development were dark-adapted for 14 h. Electroretinography (ERG) recordings were performed in anesthetized animals essentially as described by Phillips *et al.* (28) using an Espion $E^2$ system and ColorDome Ganzfeld Stimulator (Diagnosys, Lowell, MA, USA). Recordings were performed using an intensity/response series of 12 4 ms flashes ranging from 0.001 to 100 cd.s/$m^2$ in intensity (29, 30).

### Test of spatial visual function

Spatial frequency (sf) thresholds for opto-kinetic tracking of a sine-wave grating were measured in C57BL/6J 4-mo-old offspring using a virtual optokinetic system (OptoMotry; Cerebral Mechanics, Medicine Hat, AB, Canada) (31, 32). A vertical sine-wave grating moving at 12°/s or gray of the same mean luminance were projected on 4 monitors as a virtual cylinder that surrounded an unrestrained mouse standing on a platform at the epicenter. The hub of the cylinder was continually centered between the eyes of the mouse to precisely set the sf of the grating at the mouse's viewing position as it shifted its body position. Gray was projected while the mouse was moving, but when movement ceased, the gray was replaced with the grating. Grating rotation elicited reflexive tracking behavior, which was scored *via* live video image using a method of limits staircase procedure with a yes/no criterion. Sf thresholds were determined for each eye independently by changing the direction of grating movement: clockwise movement (left eye) and counterclockwise (right eye) (32). Obtained sf thresholds were manually confirmed at the end of the testing period. The investigator conducting the testing was blinded to the animal's experimental group.

### Tissue collection

Embryos were decapitated, brains were removed, and embryonic heads were fixed in 4% paraformaldehyde/1 time PBS overnight at 4°C. For histology and immunohistochemistry in adult animals, eyeballs were collected from animals euthanized using $CO_2$ and fixed in 4% paraformaldehyde/1 time PBS overnight at 4°C. Tissues were dehydrated in sucrose/1 time PBS solution at 4°C, with increasing sucrose concentrations (10–30%) over 48 h. Tissues were mounted in OCT compound (Thermo Fisher Scientific, Waltham, MA, USA), frozen on dry ice, and stored at −80°C. Embryonic heads were cryosectioned coronally at 20 μm such that each consecutive section was adhered to one of the consecutive slides in a series of 7, equally distributing tissues of each sample over a series of 7 slides. Slides were stored at −20°C.

### Histology

Hematoxylin and eosin staining was performed on 20-μm-thick retinal frozen sections. Briefly, slides were dried at room temperature for at least 1 h and rinsed in 2 changes of running tap water. Gills hematoxylin was added to slides for 3.5 min, followed by 2 rinses in running tap water. Slides were dipped 3–4 times in lithium carbonate and rinsed in tap water. Slides were dipped 10 times in 95% ethanol. Eosin was applied for 30 s, followed by 2 rinses in 95% ethanol, 2 rinses in 100% ethanol, and 3 rinses in xylene.

### Toluidine blue staining and transmission electron microscopy

Mouse eyes were immersion-fixed in 2% paraformaldehyde/2.5% glutaraldehyde/0.1 M sodium cacodylate, pH 7.4, and stored at 4°C for several days before enucleation. The eyecups were washed 3 × 10 min with 0.1 M sodium cacodylate buffer followed by postfixation in 1% osmium tetroxide/0.1 M sodium cacodylate buffer, pH 7.4, for 1 h. After washing with deionized water (3 × 15 min), the eyecups were stained *en bloc* with 2% aqueous uranyl acetate for 30 min, rinsed in water, and dehydrated with increasing concentrations of ethanol (30, 50, 75, 90, 100, and 100% at 15 min each). Following two 15-min changes of propylene oxide, the samples were infiltrated overnight with a 1:1 mixture of propylene oxide and PolyBed 812/Spurr's epoxy resin (Polysciences, Warrington, PA, USA). After 2 changes in 100% PolyBed 812/Spurr's resin (8 h, then overnight), the eyecups were embedded in fresh resin and blocks were polymerized overnight at 60°C. The eyecups were sectioned transversely close to midline (from optic nerve to cornea) with a diamond knife at 1 μm thickness, mounted on slides, and stained with 1% toluidine blue in 1% sodium borate. Slides were examined and photographed with an Olympus BX-61 microscope (Olympus America, Center Valley, PA, USA) equipped with a Retiga 4000R CCD camera (Teledyne QImaging, Surrey, BC, Canada) and Volocity v6.3 software (PerkinElmer, Waltham, MA, USA). Comparable regions of interest were selected, and ultrathin sections (70–80 nm) were cut with a diamond knife, mounted on 200 mesh copper grids followed by staining with 4% aqueous uranyl acetate for 12 min and Reynolds' lead citrate for 8 min. Grids were observed using a JEOL JEM-1230 transmission electron microscope operating at 80 kV (Jeol USA, Peabody, MA, USA) and images were acquired with a Gatan Orius SC1000 CCD Digital Camera and Gatan Microscopy Suite 3.0 software (Gatan, Pleasanton, CA, USA).

### Immunohistochemistry

Slides were dried at room temperature for 1 h, hydrated in 1 time PBS, and incubated in blocking solution containing 2% goat or donkey serum (Thermo Fisher Scientific) and 0.01% Triton X-100 (MilliporeSigma, Burlington, MA, USA) in 1 time PBS for 1 h. Antigen retrieval for immunostaining against bromodeoxyuridine (BrdU), iododeoxyuridine (IdU), Ki67, and phosphohistone 3 (PH3) was performed by steaming the slides in a solution containing 10 mM sodium citrate, 0.05% Tween 20 (pH 6.0) for 20 min prior to the incubation in blocking solution. Slides were incubated in blocking solution containing primary antibodies overnight at 4°C. The following antibodies and dilutions were used: rat anti-BrdU (1:100, ab6326; Abcam, Cambridge, MA, USA), mouse anti-BrdU/IdU (1:100, 347580; BD Biosciences, San Jose, CA, USA), rabbit anti-Calbindin (1:1000, ab11426; Abcam), rabbit anti-Calretinin (1:1000, MAB1568; Thermo Fisher Scientific), rabbit anti-cleaved Caspase 3 (1:50, 9579; Cell Signaling Technology, Danvers, MA, USA), goat anti-ChAT (1:30, AB144P; MilliporeSigma), rabbit anti-cone arrestin (1:250, AB15282; MilliporeSigma), chicken anti-EGFP (1:1000, ab290; Abcam), mouse anti-ISL LIM Homeobox 1 (Islet1) (1:50, 40.3A4; Developmental Studies Hybridoma Bank, Iowa City, IA, USA); rabbit anti-Ki67 (1:500, ab15580; Abcam), mouse anti-Nestin (1:150, 14-5843-82; Thermo Fisher Scientific), goat anti-Otx2 (1:500, 1979; R&D Systems, Minneapolis, MN, USA), rabbit anti-PH3 (1:1000, 05-636; MilliporeSigma), rabbit anti-red/green opsin (1:300, AB5405; MilliporeSigma) rabbit anti-spalt-like transcription

factor 3 (Sall3) (1:250, HPA016656; MilliporeSigma), Click-It EdU Detection Kit (C10337; Thermo Fisher Scientific) was used to detect 5-ethynyl-2′-deoxyuridine (EdU). Lectin PNA Alexa647 (1:250, B-1075; Vector Laboratories, Burlingame, CA, USA) was used to detect cone outer segments. The following secondary antibodies were used: goat anti-chicken Alexa 647 (1:500; Jackson ImmunoResearch Laboratories, West Grove, PA, USA), goat anti-mouse Alexa 488 (1:1000; Jackson ImmunoResearch Laboratories), goat anti-rabbit CY3 (1:250; Jackson ImmunoResearch Laboratories) goat anti-rat Alexa 488 (1:2000; Thermo Fisher Scientific), goat anti-mouse Alexa 555 (1:2000; Thermo Fisher Scientific), donkey anti-goat Alexa 488 (1:1000; Jackson ImmunoResearch Laboratories). DAPI (1:4000; MilliporeSigma) was used to label cell nuclei. Images were acquired using an LSM710 laser scanning confocal microscope (Carl Zeiss, Oberkochen, Germany). *Z* stacks with 5–7 optical slices through 14–20 μm were obtained from tissue sections or whole-mounted retinas. Image analysis was performed using ImageJ software (National Institutes of Health, Bethesda, MD, USA).

### Cell quantification

For embryonic studies, both retinas from at least 3 embryos and at least 3 distinct litters were used for analyses. Cells were manually counted on *z*-stacks collected at 20 or 40 times from 20 μm sections using ImageJ software. The following regions of interest were used: oligodendrocyte transcription factor 2 (Olig2) E17.5 100 μm × 100 μm; Olig2 E14.5 170 μm × 170 μm; Otx2 70 μm × 70 μm; PH3, EdU/Ki67, Islet1, Sall3, Calbindin, 100 μm × 100 μm; peanut agglutinin (PNA) 200 × 200 μm. Quantification of retinal thickness was performed on immunofluorescent images of comparable central regions of adequate choline and low choline retinas and in central retinal regions on histologic images of adequate and low choline retinas.

### Cell cycle analysis

Pregnant dams (d 14.5 of pregnancy) were injected intraperitoneally with IdU (120 mg/kg body weight) at time 0 ($T_0$). At $T_1$ = 1.5 h, dams were injected with BrdU (100 mg/kg body weight; Sigma B5002; MilliporeSigma). At $T_2$ = 2 h, dams were culled and embryonic heads were fixed in cold 4% PFA. Mouse antibody against IdU and BrdU was used to detect both thymidine analogs, and a rat antibody specific to BrdU (Bio-Rad, Hercules, CA, USA) was used to detect BrdU alone (33, 34). The following formulas were used to calculate the lengths of the S-phase ($T_S$) and the entire cell cycle ($T_C$):

$$T_S = T_1/(\mathrm{IdU}^+;\mathrm{BrdU}^-\,\mathrm{cells}/\mathrm{IdU}^-;\mathrm{BrdU}^+\,\mathrm{cells})$$

$$T_C = T_S/(\mathrm{IdU}^-;\mathrm{BrdU}^+\,\mathrm{cells}/\mathrm{Ki67}^+\,\mathrm{cells})$$

### Western blot

Retinas were collected from E17.5 embryos and lysed on ice in RIPA buffer supplemented with protease inhibitor cocktail (Roche, Basel, Switzerland) using sonication. Total protein concentration for all samples was quantified using the BCA assay (Bio-Rad). Proteins were loaded into SDS-PAGE gels and blotted on PVDF membranes. Immunolabeling was accomplished using the following antibodies: Yes-associated protein (YAP)/tafazzin (TAZ) (8418; Cell Signaling Technology), PAK1 (2602; Cell Signaling Technology), and NF2 (MABN1786; MilliporeSigma, Burlington, MA, USA). The secondary antibodies were goat anti-rabbit 800 CW (925–32211; Li-Cor Biosciences, Lincoln, NE, USA) and goat anti-mouse 600 RD (925–68070; Li-Cor Biosciences). The membranes were imaged in Li-Cor Odyssey imaging system.

### Statistical analyses

Data were analyzed with respect to normal distribution and presence of outliers using Prism 6 software (GraphPad Software, La Jolla, CA, USA). Cell densities were compared using 2-tailed Student's *t* test; cell proportions were compared by Mann-Whitney test. For the ERG data, we calculated the average amplitude between the 2 eyes and the difference in the amplitudes between the 2 eyes. The average and difference data were analyzed separately using a mixed linear model followed by pairwise comparison between the 2 treatments (low choline *vs.* adequate choline) at each light intensity level. Pairwise comparison was performed using Student's *t* test. The distribution of the data was examined for normality and equal variance assumptions. Log transformation was performed for the difference data to meet the normality assumption. Levene's test was used to examine the equal variance assumption; when *P* value was significant, Welch *t* test was used to replace Student's *t* test. Benjamini-Hochberg procedure for false discovery rate control (35) was used to correct the *P* values from multiple tests. Data sets with more than 1 group were analyzed using 1-way ANOVA. Data are shown as means ± SEM unless specified otherwise in figure legends.

## RESULTS

### Low choline availability during gestation leads to persistent retinal structural defects

Through its role in the regulation of NPC proliferation and differentiation, choline is important for supporting the proper temporal progression of neurogenesis in the cerebral cortex (12, 14). To determine whether low availability of choline during development also affects the final cellular organization of the retina, we evaluated retinal gross morphology in low choline and adequate choline offspring at various ages, ranging from P35 to 1 yr of age (Supplemental Tables S1 and S2). Histologic examination revealed that the majority of retinas in animals exposed to low choline diet between E11.5 and E17.5, or between E11.5 and P3, exhibit structural abnormalities (**Fig. 1*A* *vs.* *B–D***). The most common defects observed in low choline retinas are lesions characterized by the focal displacement of retinal neuronal cells, photoreceptor cells in particular, into subretinal space and associated with regions of retinal thinning (Fig. 1*E*, large arrow; Fig. 1*F*, arrow). In addition, we find that 18% of low choline retinas that do not exhibit obvious lesions are hypocellular (Fig. 1*C* and Supplemental Fig. S1 and Supplemental Table S2). Lesions were not observed in adequate choline retinas (Supplemental Tables S1 and S2). A longer period of low choline availability, E11.5-P3, results in severe retinal disorganization in a subset of animals (4 out of 8 retinas examined) (Fig. 1*D*). In addition, immunohistochemical (Fig. 1*G*, red arrows) and histologic examination (Fig. 1*H*, black arrows) reveals the presence of abnormally large blood vessels in low choline compared to adequate choline retinas. Structural abnormalities in low choline retinas are observed in animals raised on 3 types of defined diets (see Materials and Methods), and do not appear to become exacerbated with age, as 16-mo-old low choline animals examined in this study still display a single lesion (Supplemental Table S1). Overall, 68% of low choline retinas exhibit abnormal retinal structural architecture (summarized in Supplemental Table

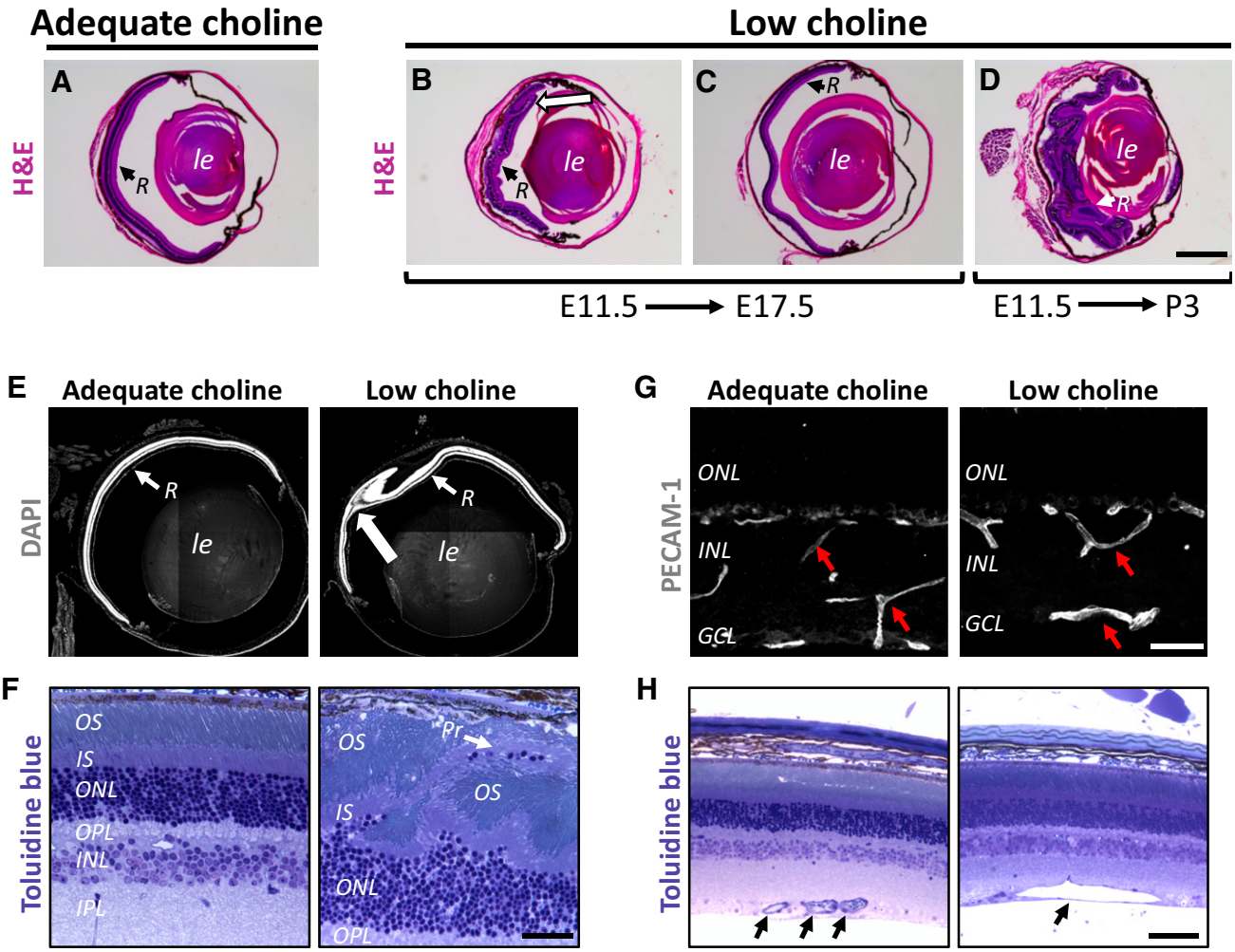


**Figure 1.** Cytoarchitectural abnormalities in adult low choline retinas. *A*) Normal retinal gross morphology in adult adequate choline animals, revealed by hematoxylin and eosin staining. *B*, *C*) Cytoarchitectural abnormalities, such as retinal folding [(*B*), white arrow] and hypocellularity (*C*) are observed in retinas of animals exposed to low choline diet between E11.5 and E17.5. *D*) Extensive disruption of retinal organization is observed in a subset of low choline animals exposed to low choline diet between E11.5 and P3. *E*) Focal displacement of retinal cells into subretinal space, revealed by DAPI staining, is the most commonly observed defect in low choline retinas (large white arrow) (also see Supplemental Table S1). *F*) Toluidine blue staining of semithin retinal sections reveals disorganization of photoreceptor inner and outer segments in the areas of focal dysgenesis in low choline retinas and displacement of photoreceptor cell bodies into subretinal space (white arrow). *G*) Immunostaining against PECAM-1 shows presence of abnormally large blood vessels in low choline compared to adequate choline retinas. *H*) Example of an abnormally large blood vessel in low choline retina compared to normal size blood vessels in adequate choline retina (black arrows). INL, inner nuclear layer; IPL, inner plexiform layer; IS, inner segments; low le, lens; OPL, outer plexiform layer; OS, outer segment; PECAM-1, platelet endothelial cell adhesion molecule 1; Pr, photoreceptor; R, retina. Scale bars, 750 μm (*B*), 600 μm (*E*), 120 μm (*F*), 120 μm (*G*), 200 μm (*H*).

S2). Together, these data show that low maternal intake of choline during pregnancy results in retinal structural defects in the offspring, ranging from hypocellularity to lesions occurring due to displacement of retinal neurons into subretinal space.

## Abnormal photoreceptor ultrastructure in low choline retinas

Cone photoreceptor function is essential for daylight vision (36, 37). To evaluate whether structural abnormalities in adult low choline animals are associated with abnormal cone photoreceptor cell organization or morphology, we first compared the final density of cone photoreceptors between adequate choline and low choline adult offspring. Using lectin PNA staining, we determined that the densities of cone outer segments are not different between adequate choline and low choline adult offspring (Supplemental Fig. S1*A*, *B*). However, cone outer segments appeared disorganized in retinal regions devoid of lesions (**Fig. 2*A* *vs.* 2*B***), and the organization of the entire outer nuclear layer (ONL) was significantly altered in the regions of low choline retinas that did display lesions (Fig. 2*C*, *D* *vs.* Fig. 2*A*, large arrow). Immunostaining of flat-mounted retinas against red/green opsin revealed abnormal distribution of red/green opsin within cone outer segments in low choline retinas (Fig. 2*E*, red). Similarly, localization of red/green opsin in PNA-labeled cone outer segments examined in retinal sections appeared discontinuous and irregular in low choline compared to adequate choline animals (Fig. 2*F*, insets). Localization of cone arrestin in low choline retinas also exhibited an irregular pattern

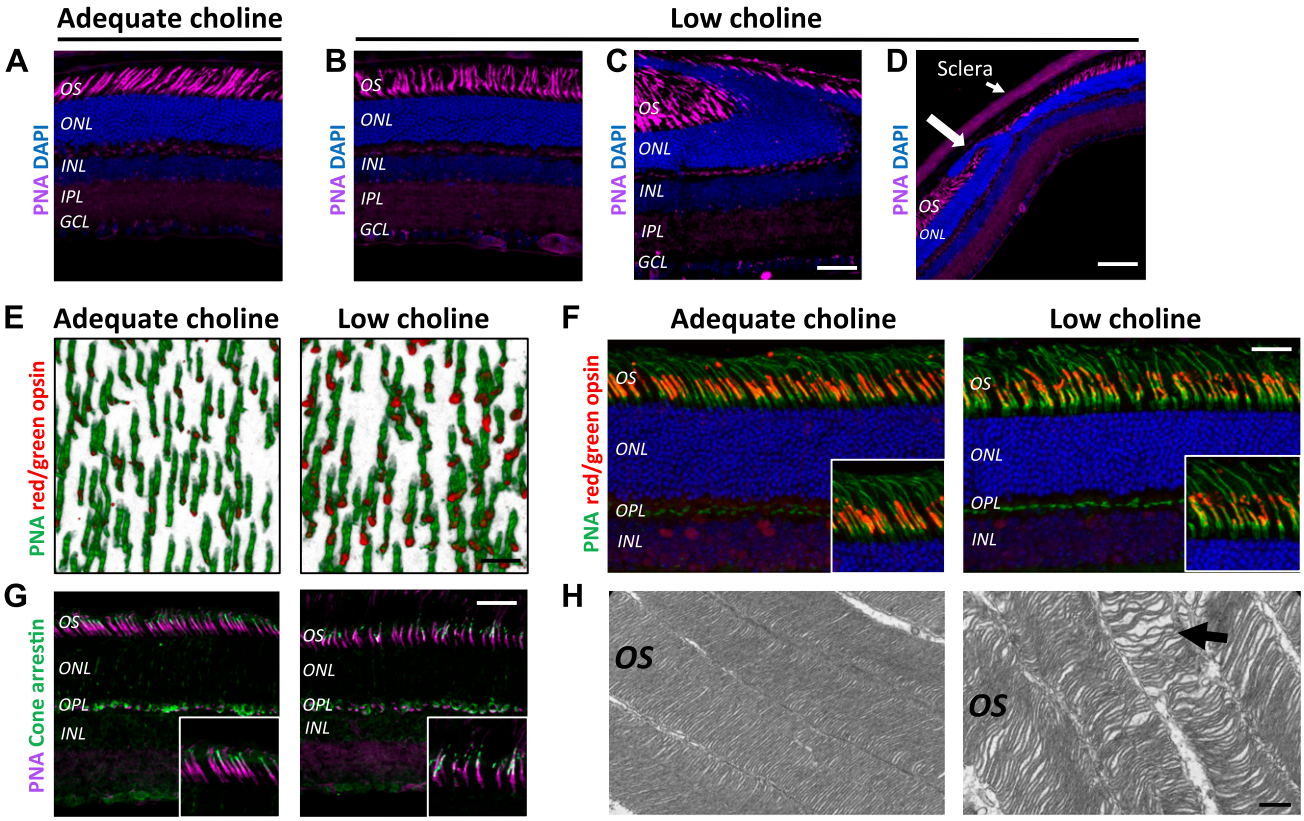


**Figure 2.** Photoreceptor outer segment integrity is compromised in adult animals exposed to low choline availability between E11.5 and E17.5. *A*, *B*) Compared to cone photoreceptor outer segments, labeled by PNA, in 4-mo-old adequate choline animals (*A*), cone outer segments in low choline retinas (regions devoid of structural defects) appear disorganized (*B*). *C*, *D*) Retinal folding and protrusion of photoreceptors into subretinal space in low choline retinas compromises outer segment organization (*C*) and ONL integrity ((*D*), large arrow). *E*) Immunostaining against red/green opsin (red) and lectin PNA (green) in flat-mounted adequate and low choline retinas (3-dimensional rendering) shows enlarged areas of red/green opsin immunoreactivity in low choline cone outer segments. *F*) Aberrant red/green opsin localization is observed in lectin PNA-labeled cone outer segments in cross sections of low choline compared to adequate choline retinas (insets). *G*) Aberrant localization of cone arrestin is detected in lectin PNA-labeled cone outer segments of low choline compared to adequate choline retinas. *H*) Transmission electron microscopy images reveal that organization of photoreceptor outer segment membrane discs is less compact in low choline compared to adequate choline retinas (black arrows) ($n$ = 2 males and 2 females per group). INL, inner nuclear layer; IPL, inner plexiform layer; IS, inner segments; OPL, outer plexiform layer; OS, outer segment. Scale bars, 70 μm (*C*), 160 μm (*D*), 70 μm (*E*), 70 μm (*F*), 70 μm (*G*), 0.5 μm (*H*).

compared to adequate choline retinas (Fig. 2*G*, insets). Finally, ultrastructural examination of photoreceptor outer segments using transmission electron microscopy revealed that membrane disks of photoreceptor outer segments are less tightly organized in low choline compared to adequate choline retinas (Fig. 2*H*, arrow). These results demonstrate that low choline availability during development leads to lasting defects in photoreceptor outer segment organization and ultrastructure.

## Differentiation of retinal neurons is inhibited due to low supply of choline *in utero*

To determine the temporal stage at which low choline diet induces structural retinal disorganization, and the possible cause for retinal hypocellularity, we examined retinas of E17.5 embryos exposed to low choline or adequate choline maternal diets between E11.5 and E17.5 using immunohistochemistry (**Fig. 3**). We found that only a small fraction of low choline E17.5 embryos (4 out of >20) exhibited displacement of retinal cells into subretinal space (Supplemental Fig. S2), suggesting that the structural defects and lesions that we observe in adult low choline retinas arise predominantly during postnatal development. We next examined the densities of retinal neurons born during prenatal stages of retinogenesis (Fig. 3*A*): RGCs and a subset of amacrine cells marked by the expression of Islet1, horizontal cells marked by Sall3, and cone photoreceptor precursors marked by Otx2 expression, in adequate choline and low choline E17.5 retinas. We found that the densities of Islet1-expressing cells in the presumptive ganglion cell layer (GCL) are reduced in low choline *vs.* adequate choline retinas (Fig. 3*B vs.* 3*C*, *D*; $P$ = 0.0002 by Student's $t$ test). Similarly, densities of Sall3-expressing differentiating horizontal cells (Fig. 3*E–G*; $P$ = 0.03 by Student's $t$ test) and Otx2-expressing cone photoreceptor precursors in the outer neuroblastic cell layer (NBL) (Fig. 3*H–J*; $P < 0.0001$ by Student's $t$ test) are reduced in low choline (Fig. 3*F*, *I*) *vs.* adequate choline (Fig. 3*E*, *H*) E17.5 retinas. Consistent with the reduction in the densities of amacrine and horizontal cells, expression of calbindin, another marker of differentiating

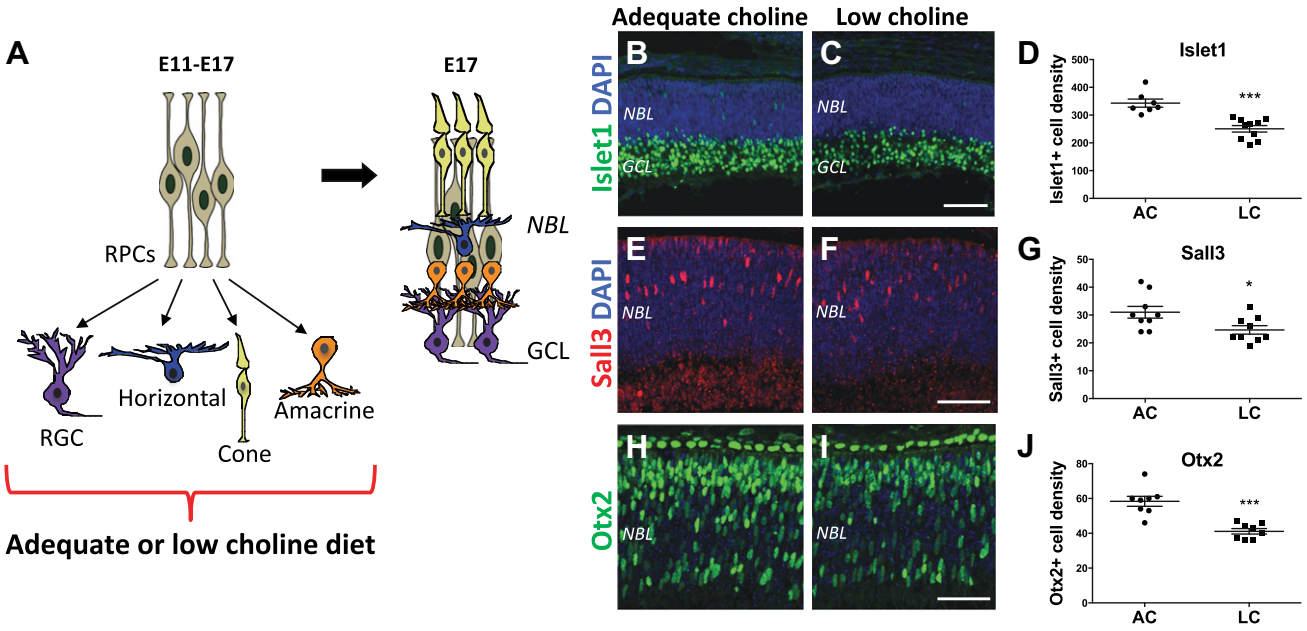


**Figure 3.** Neuronal differentiation is disrupted in E17.5 low choline retinas. *A*) Schematic diagram illustrating neuronal daughter cells produced by RPCs during the period of low or adequate choline diet administration between E11.5 and E17.5 and their spatial organization in the E17.5 retina. *B–D*) Expression of Islet1, marking RGCs and a subset of amacrine cells, is reduced in the presumptive GCL of low choline (LC; $n = 10$) (*C*) compared to adequate choline (AC; $n = 7$) (*B*) E17.5 retinas [(*D*); $P = 0.0002$ by Student's *t* test]. *E–G*) Density of Sall3-expressing differentiating horizontal cells in the NBL is reduced in LC ($n = 9$) (*F*) *vs.* AC ($n = 9$) (*E*) E17.5 retinas [(*G*); $P = 0.03$ by Student's *t* test]. *H–J*) Density of Otx2-expressing cone photoreceptor precursors is reduced in LC ($n = 8$) (*I*) compared to AC ($n = 8$) (*H*) E17 retinas [(*J*); $P < 0.0001$ by Student's *t* test]. Scale bars, 100 μm (*C*, *F*), 70 μm (*I*). ***$P < 0.001$, *$P < 0.05$ by Student's *t* test.

amacrine and horizontal cells, is also reduced in low choline compared to adequate choline retinas at E17.5 (Supplemental Fig. S3*A*, *B*). Importantly, we did not detect appreciable numbers of activated caspase 3–positive apoptotic cells in low choline or adequate choline E17.5 retinas that would warrant cell quantification (Supplemental Fig. S3*C–F*), nor did we observe appreciable numbers of pyknotic nuclei, suggesting that cell death may not be the principle reason for the reduction in differentiating neurons in E17.5 low choline retinas. Together, these results demonstrate that differentiation of retinal neurons born during embryonic period of retinal development is inhibited due to low supply of choline in maternal diet, whereas the onset of structural dysgenesis in the majority of low choline retinas occurs later than E17.5.

## Low availability of choline increases the proportion of RPCs compared to differentiating cells in E17.5 retinas

To confirm our observation that low supply of choline reduces RPC differentiation, we determined the relative proportions of RPCs and differentiating neurons in low choline *vs.* adequate choline E17.5 retinas (**Fig. 4**). To this end, we used expression of NestinCFP in *NestinCFP*$^{+/-}$ transgenic embryos to distinguish between NestinCFP-expressing RPCs and differentiating neurons, which down-regulate NestinCFP expression (12, 25). We first confirmed that NestinCFP is expressed strictly in RPCs, evidenced by its expression in the NBL and not in the presumptive inner nuclear layer/GCL, marked by the expression of calretinin and containing differentiating neurons (Fig. 4*A*). Next, we dissociated adequate choline and low choline E17.5 retinas into single cells and determined the relative proportions of NestinCFP-positive and NestinCFP-negative cells between the groups (Fig. 4*B*). We found that the proportions of NestinCFP- as well as Nestin protein–expressing RPCs, relative to NestinCFP- and Nestin protein–negative cells, are increased in low choline compared to adequate choline retinas (Fig. 4*C*, *D*). Importantly, expression of NestinCFP in relation to Nestin protein remains unchanged in low choline *vs.* adequate choline E17.5 retinas, suggesting that low choline availability does not affect the expression of *NestinCFPnuc* transgene itself (Fig. 4*E*). These results suggest that a decrease in differentiating neurons in low choline retinas is accompanied by an increase in the relative proportions of Nestin-expressing RPCs.

During the embryonic period of mouse retinal development, a subset of RPCs expressing Olig2 transcription factor produce predominantly cone photoreceptors and horizontal cells (Fig. 4*F*) (38). We therefore sought to determine whether, consistent with an increase in relative RPC proportions, the densities of Olig2-expressing RPCs may be also increased in low choline embryos. Using immunostaining against Olig2, we found that the densities of Olig2-expressing RPCs remain comparable between low choline and adequate choline retinas at E14.5 (Fig. 4*G*, *H*). However, at E17.5, Olig2-expressing RPC density is increased in low choline compared to adequate choline retinas (Fig. 4*I*, *J*). In addition, using immunostaining against calbindin to

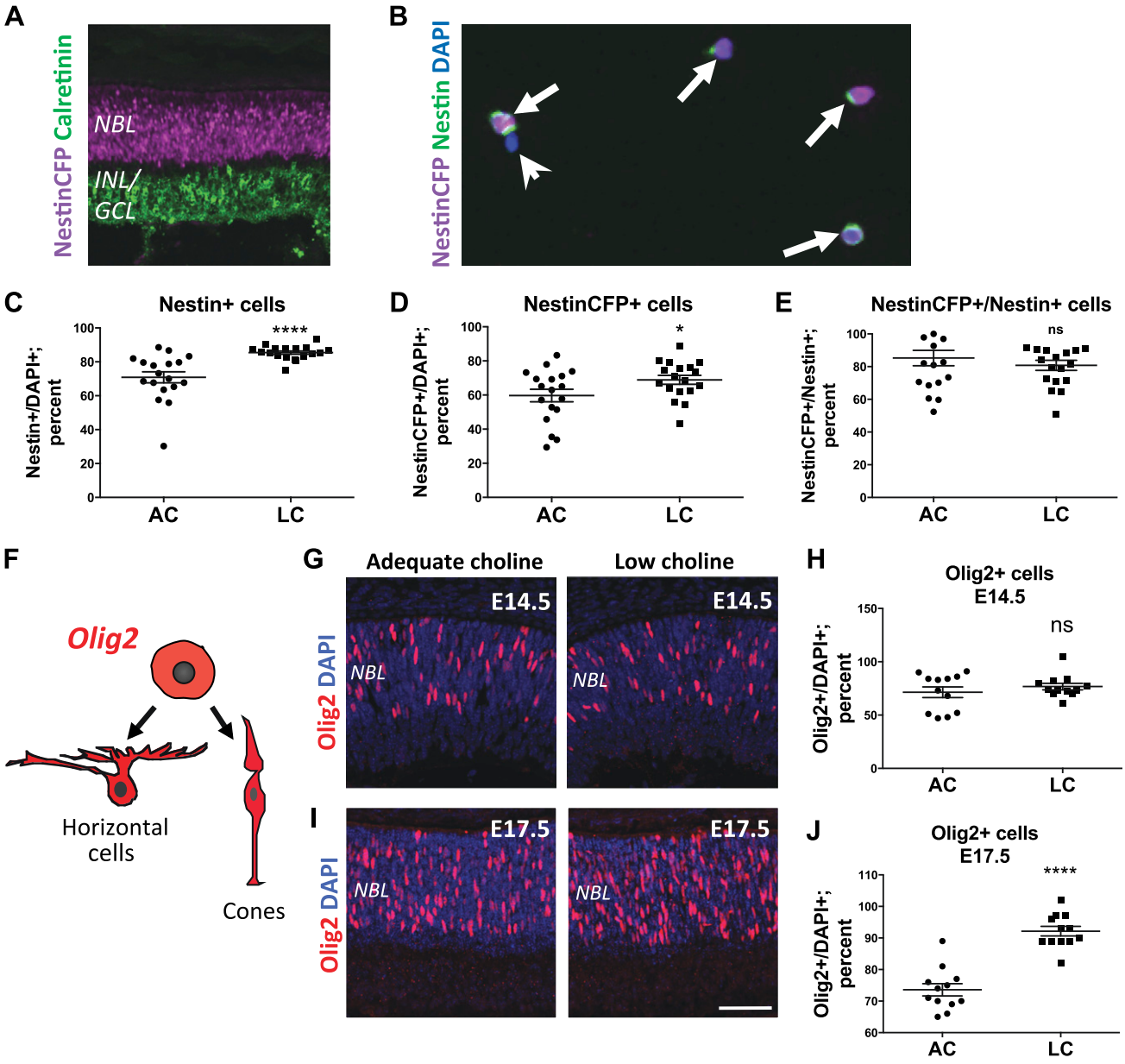


**Figure 4.** Relative proportions of RPCs are increased in low choline (LC) compared to adequate choline (AC) E17.5 retinas. *A*) Nuclear expression of NestinCFP (purple) in *Nestin-CFPnuc*$^{+/-}$ transgenic E17.5 embryos is restricted to the majority of RPCs in the NBL and is not detected in the presumptive inner nuclear layers/GCLs marked by the expression of calretinin (green). *B*) Immunostaining of dissociated E17.5 *Nestin-CFPnuc*$^{+/-}$ retinas against NestinCFP (purple) and endogenous Nestin protein (green) allows for identification of RPCs (arrows) and differentiating neurons that no longer express Nestin (arrowhead). *C, D*) Proportions of Nestin-expressing cells [(*C*); $P < 0.0001$ by Mann-Whitney test] and NestinCFP-expressing cells [(*D*), $P = 0.05$ by Mann-Whitney test] are increased in LC ($n = 18$) compared to AC ($n = 18$) dissociated retinas. *E*) The ratios of NestinCFP-expressing to Nestin-expressing cells are not different between AC and LC retinas. *F*) Schematic diagram illustrating a subset of daughter cells, cone photoreceptors and horizontal cells, produced by Olig2-expressing RPCs during embryonic mouse retinogenesis. *G, H*) At E14.5, the densities of Olig2-expressing RPCs (red) in the NBL of AC ($n = 12$) and LC ($n = 12$) retinas (*G*) are not significantly different (*H*). *I, J*) At E17.5, the density of Olig2-expressing RPCs (*I*) is increased in LC ($n = 12$) compared to AC ($n = 12$) retinas [(*G*); $P < 0.0001$ by Student's *t* test]. *INL*, inner nuclear layer; ns, not significant. Scale bar, 100 μm (*I*). $^{*}P < 0.05$, $^{****}P < 0.0001$.

identify horizontal cells in the outer plexiform layer, we determined that the final density of horizontal cells remains reduced in adult low choline compared to adequate choline retinas (Supplemental Fig. S1C, *D*). These data show that increased proportions of RPCs in E17.5 low choline retinas are associated with a decrease in differentiating neurons, suggesting that differentiation capacity of low choline RPCs may be altered.

## Reduced neuronal differentiation in low choline retinas is accompanied by the maintenance of RPC identity

Following cell division, RPC daughter cells either maintain progenitor cell identity and progress through another round of cell division or exit the cell cycle and acquire neuronal fate. To determine whether low choline RPC

differentiation following cell division could be inhibited, we used genetic lineage tracing. Specifically, we generated *Nestin-CreER*$^{T2+/-}$; *Ai9*$^{+/-}$ double-transgenic embryos, in which activation of Cre recombinase is regulated by tamoxifen (TM) and results in permanent expression of Cre reporter, tdTomato fluorescent protein, from the *Ai9* Cre reporter allele in *NestinCreER*$^{T2}$-expressing RPCs and all their progeny (**Fig. 5*A***) (14, 26). Next, we activated Cre recombinase in *Nestin-Cre*$^{ERT2+/-}$; *Ai9*$^{+/-}$ adequate choline and low choline pregnant females by a single injection of TM at E14.5 and analyzed the resulting progeny labeled by the expression of tdTomato at E18.5 (Fig. 5*B*). Based on cell morphology, retinal layer position, as well as radial alignment of clonally related RPCs, described in the literature (38, 39), we classified single labeled cells and groups of cells into 4 categories: *1*) single neurons (N), *2*) groups of RPCs with fewer than 4 cells ($P \leq 4$), *3*) groups of RPCs with more than 4 cells ($P > 4$), and *4*) undefined (U) (Fig. 5*C*). Analysis of tdTomato labeled cells revealed a larger proportion of groups of RPCs containing more than 4 cells ($P > 4$) (Fig. 5*D*, *E*; $P = 0.01$ by Mann-Whitney test), as well as all groups of RPCs ($P > 4$ and $P \leq 4$) (Fig. 5*D*, *F*; $P = 0.02$ by Mann-Whitney test), in low choline *vs.* adequate choline retinas among all observed recombination events. These data suggest that a subset of low choline RPCs maintains progenitor cell identity following cell division, further confirming that RPC differentiation in low choline retinas is inhibited.

## Disruption of RPC cell cycle dynamics and down-regulation of neurofibromin 2 protein in low choline retinas

To determine whether aberrant cell cycle dynamics contributes to the observed reduction in retinal neurons and increased proportions of RPCs in low choline retinas, we examined the length of the S-phase and the entire cell cycle length in adequate choline *vs.* low choline RPCs. To achieve this, we labeled RPCs undergoing S-phase of the cell cycle by administering the thymidine analog IdU to E14.5 pregnant females at $T_1$ (0 h), followed by the administration of another thymidine analog BrdU 30 min later at $T_2$ (0.5 h) and euthanizing animals 1.5 h following BrdU administration at $T_3$ (1.5 h) (**Fig. 6*A***) as previously described (38, 39) (see Materials and Methods). IdU and BrdU can be distinguished using antibodies specific to either IdU alone or recognizing both IdU and BrdU (33, 34). Cells labeled with IdU alone represent RPCs that have completed the S-phase of the cell cycle and have moved on to G2 and M phases (Fig. 6*A*). In accordance with interkinetic nuclear migration, which places cell bodies of mitotic RPCs strictly at the apical retinal surface (40), we find that IdU singly-labeled nuclei are located primarily at the outer retinal boundary in adequate choline retinas (Fig. 6*B*, arrows). Surprisingly, very few IdU singly-labeled cells are detected in low choline retinas (1 cell in each of the 3 out of 12 retinal sections examined, representing both retinas of 3 embryos from 3 distinct litters) (Fig. 6*B*). Accordingly, we find that the length of the S-phase of the cell cycle ($T_S$) (Fig. 6*C*), as well as the entire cell cycle length ($T_C$) (Fig. 6*D*), are increased in low choline compared to adequate choline RPCs. These results suggest that completion of DNA synthesis during the S-phase of the cell cycle in low choline RPCs is delayed while the entire cell cycle length is increased.

Consistent with delayed completion of the S-phase, fewer mitotic RPCs marked by the expression of PH3 are observed in low choline compared to adequate choline retinas at E17.5 (Fig. 6*E*, *F*; $P < 0.0001$ by Student's *t* test). To confirm that cell cycle exit of low choline RPCs remains compromised at E17.5, we labeled RPCs undergoing DNA synthesis during the S-phase of the cell cycle at E16.5 by injecting pregnant females with thymidine analog, EdU, and evaluated the numbers of EdU-positive cells coexpressing Ki67 24 h later, at E17.5 (Fig. 6*G*). We found that the proportion of RPCs that remain in the cell cycle, as determined by the proportion of EdU/Ki67 double-positive cells among Ki67-expressing cells, is higher in low choline compared to adequate choline E17.5 retinas (Fig. 6*H*; $P = 0.004$ by Mann-Whitney test). These results demonstrate that the increase in RPC cell cycle length may contribute to reduced neuronal differentiation in low choline retinas.

Neurofibromin 2 (Nf2)/Merlin protein is an upstream regulator of the Hippo signaling pathway and couples regulation of cell cycle progression with cell-cell adhesion (41, 42). Loss of *Nf2* function leads to persistent cell proliferation as well as disruption of adherens junction stability. We found that Nf2 protein expression is significantly reduced in E17.5 low choline compared to adequate choline retinas (Fig. 6*I*, *J*; $P < 0.0001$ by Student's *t* test), whereas the reduction in *Nf2* mRNA expression is also detected in low choline retinas at E14.5 (Fig. 6*K*; $P = 0.007$ by Student's *t* test). In addition, we detect an increase in the levels of p21-activated kinase 1 (PAK1) protein (Supplemental Fig. S4), an important regulator of Hippo signaling pathway, in low choline E17.5 retinas, whereas protein levels of Nf2 downstream effectors, YAP/TAZ transcriptional coactivators, remain unchanged (Supplemental Fig. S4). Together, these data demonstrate that aberrant differentiation of low choline RPCs is associated with an increase in RPC cell cycle length and altered expression levels of the Hippo signaling pathway regulatory proteins.

## Retinal function and visual sensitivity are altered in mice exposed to low choline diet during development

To evaluate whether observed retinal hypocellularity and presence of lesions may compromise visual function in low choline offspring, we conducted ERG recordings in dark-adapted animals exposed to either adequate choline or low choline diets between E11.5 and E17.5 using a 12-step protocol. We found that a-wave amplitudes, reflecting photoreceptor function (43), were reduced in low choline compared to adequate choline animals (**Fig. 7*A*** and Supplemental Table 3), whereas b-wave amplitudes, reflecting the function of secondary retinal neurons (44), changed significantly only at low light intensities (Fig. 7*B* and Supplemental Table S3). Moreover, longer exposure to low choline diet (E11.5-P3) further reduced the average a-wave, as well as b-wave responses, in low choline compared to adequate choline animals (Fig. 7*C*, *D*

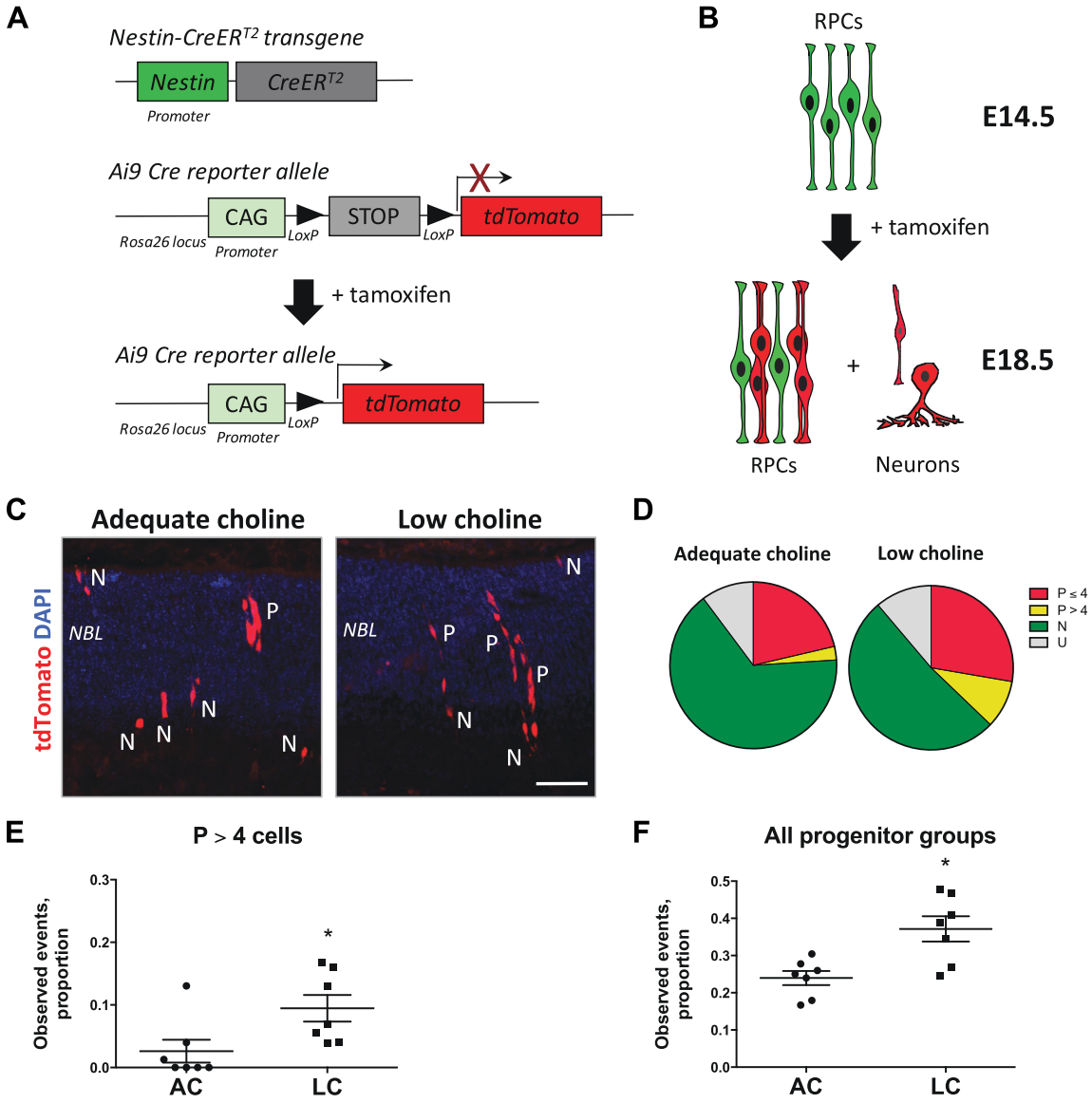


**Figure 5.** Increase in RPCs among daughter cells of *NestinCreER$^{T2}$*-expressing RPCs in low choline (LC) retinas. *A*) Schematic diagram illustrating genetic strategy of labeling daughter cells produced by RPCs with *Nestin-CreERT$^{2}$* transgene expression history in *Nestin-CreERT$^{2+/-}$; Ai9$^{+/-}$* embryos following administration of TM. Cre-mediated recombination of LoxP sites results in deletion of the stop-codon and expression of tdTomato fluorescent protein. *B*) Schematic diagram illustrating tdTomato-labeled daughter cells, including groups of radially-aligned RPCs and individual differentiating neurons, resulting from activation of Cre recombinase by TM at E14.5. *C*) Examples of tdTomato-expressing progeny in retinas exposed to adequate or LC availability between E11.5 and E18.5 following activation of Cre recombinase at E14.5. Increase in radially aligned groups of RPCs (P) is observed in LC retinas. *D*) Venn diagrams illustrating distribution of proportions of observed groups of tdTomato-expressing RPCs and individual neurons in adequate choline (AC; $n = 7$) and LC ($n = 7$) embryos. *E, F*) Increase in the proportions of RPC groups with more than 4 cells ($P > 4$) [(*E*); $P = 0.01$ by Mann-Whitney test], as well as all RPC groups ($P = 0.02$ by Mann-Whitney test), is observed in LC compared to adequate choline E18.5 retinas. CAG, cytomegalovirus (CMV) early enhancer/chicken β actin (promoter); N, neurons; P, RPCs. Scale bar, 70 μm (*C*). *$P < 0.05$ by Mann-Whitney test.

and Supplemental Table S4). Detailed examination of the data revealed a discrepancy in the a- and b-wave amplitudes between the left and the right eyes in a subset of individual low choline animals (Supplemental Fig. S5). However, the differences in a-wave and b-wave amplitudes between the 2 eyes in individual low choline animals were overall not significant (Supplemental Tables S3 and S4). Mixed model analysis, on the other hand, revealed a significant or close to significant overall diet effect in animals exposed to low choline diet between E11.5 and E17.5 ($P = 0.013$ for a-wave, and $P = 0.068$ for b-wave) and in animals exposed to low choline diet between E11.5 and P3 ($P = 0.054$ for a-wave, $P = 0.024$ for b-wave).

To address whether altered retinal function in animals exposed to low choline diets between E11.5 and E17.5 is associated with aberrant visuo-motor behavior, we examined optokinetic tracking capacity and compared sf thresholds between low choline and adequate choline animals. We first ensured that animals raised on defined diet used in our study (M-AIN93G) reach the average sf

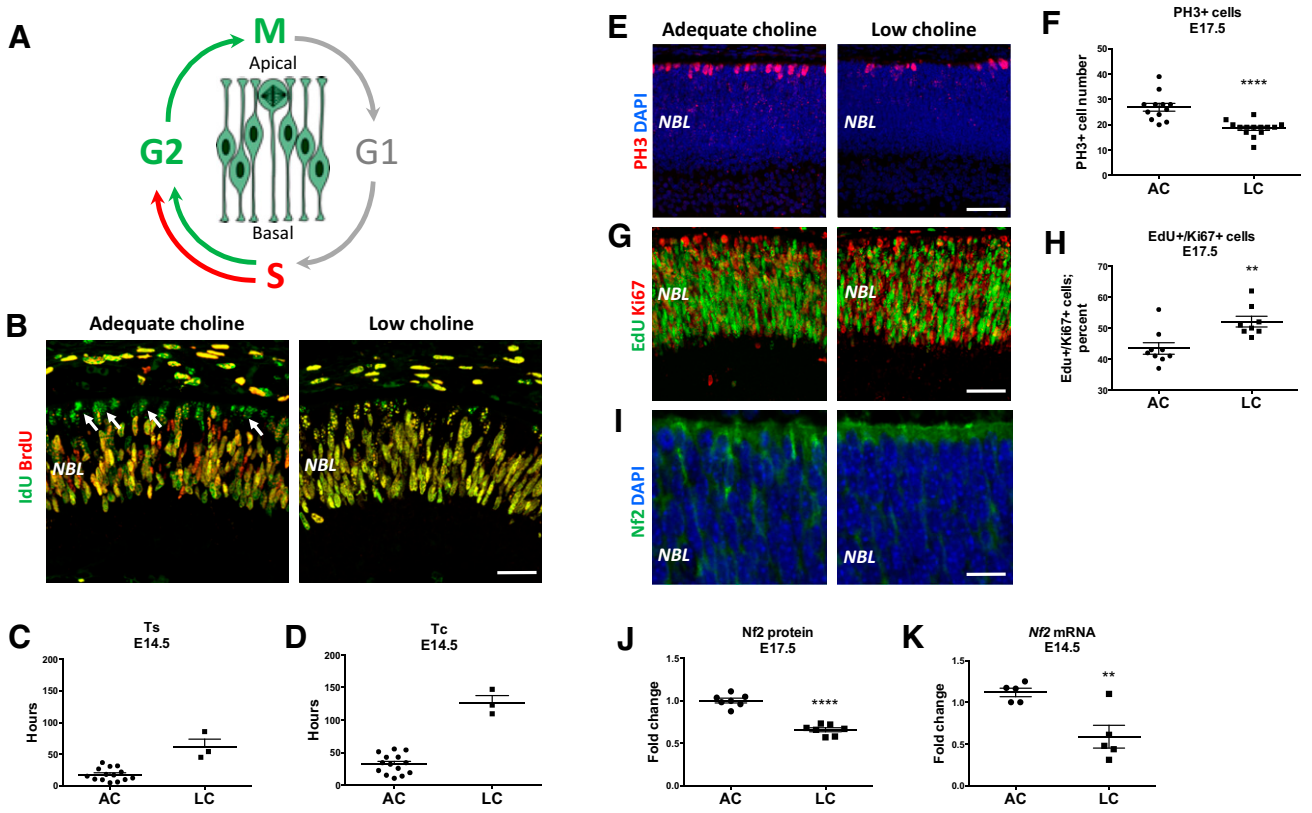


**Figure 6.** Increase in RPC cell cycle length in low choline (LC) E17.5 retinas is accompanied by down-regulation of Nf2/Merlin protein. *A*) Schematic diagram illustrating labeling of cycling RPCs by consecutive IdU and BrdU pulses. *B*) IdU singly labeled RPCs (green; arrows) are observed at the apical retinal boundary in adequate choline (AC) E14.5 embryos, whereas RPCs labeled with IdU alone are not observed in LC retinas. *C*) Calculated length of the S-phase of the cell cycle ($T_S$) (also see Materials and Methods) is increased in LC ($n = 3$) compared to AC ($n = 14$) E14.5 embryos. *D*) Calculated length of the cell cycle ($T_C$) (also see Materials and Methods) is increased in LC compared to AC E14.5 embryos. *E*, *F*) The density of mitotic RPCs expressing PH3 (red) (*E*) is reduced in LC ($n = 14$) compared to AC ($n = 12$) E17.5 retinas [(*F*); $P < 0.0001$ by Student's *t* test]. *G*, *H*) The proportion of RPCs that have incorporated EdU (green) between E16.5 and E17.5 among all RPCs expressing Ki67 (red) (*G*) is increased in LC ($n = 7$) *vs.* AC ($n = 8$) E17.5 embryos [(*H*); $P = 0.004$ by Mann-Whitney test]. *I*–*K*) Expression of Nf2/Merlin protein is reduced in LC ($n = 7$) compared to AC ($n = 7$) E17.5 retinas, revealed by immunostaining (*I*) and Western blot analyses [(*J*); $P < 0.0001$ by Student's *t* test]. *K*) Reduced levels of *Nf2* mRNA are detected in LC ($n = 5$) *vs.* AC ($n = 5$) E14.5 retinas ($P = 0.007$ by Student's *t* test). Scale bars, 55 μm (*B*), 70 μm (*E*), 70 μm (*G*), 25 μm (*I*).

threshold of 0.4 cycles per degree (c/d) observed in animals raised on chow diets and reported by others (**Fig. 8*A***) (31). Next, we compared overall sf distribution between adequate and low choline animals raised on MAIN93G diet and found that although the average sf thresholds were not different between the groups, a subset of low choline animals exhibited a notable discrepancy in sf threshold between the 2 eyes (Fig. 8*B*, red and green data points represent left and right eye sf thresholds in 2 individual animals). The average difference in sf thresholds between the left and the right eyes in individual animals is not significantly different between the groups (Fig. 8C). However, using an arbitrary sf threshold difference of 0.02 c/d, we found that 85% of low choline animals exhibited sf difference above 0.02 c/d between the 2 eyes, whereas such difference was observed in only 62% of adequate choline animals. We next analyzed sf threshold data by separating eyes with higher or lower sf thresholds reached in individual adequate choline and low choline animals (Fig. 8*D*). When we compared the average higher and lower sf thresholds, we found a significant difference in low choline male (Fig. 8*D*; $P < 0.01$ by 1-way ANOVA) and female (Fig. 8*D*; $P < 0.01$ by 1-way ANOVA) offspring, but not in adequate choline groups. Together, these data demonstrate that retinal function is altered in low choline compared to adequate choline animals, whereas visuo-motor behavior analysis shows a notable discrepancy in spatial visual sensitivity between the 2 eyes in low choline offspring.

## DISCUSSION

The importance of choline for brain development has been well established (1, 4, 19). However, to date, the role of choline availability in visual system development has not been directly examined. In this study, we addressed the requirement for choline during retinogenesis in a mouse model and determined that retinal structural integrity and function rely on adequate supply of choline during development.

Genetic loss-of-function studies in mouse models have unraveled many genes and proteins that affect development of the retina (23, 45). However, fewer environmental

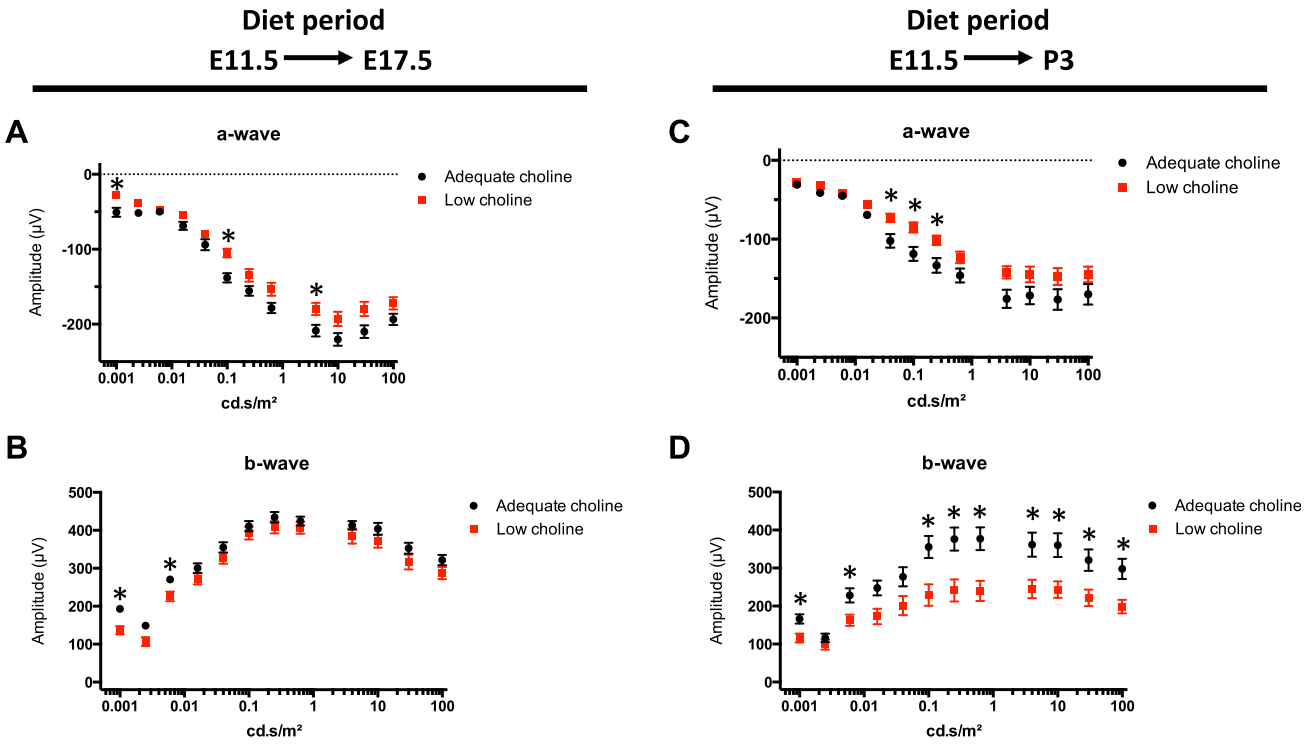


**Figure 7.** Retinal function in adult low choline offspring is altered. *A*, *B*) Amplitudes of the a-wave (*A*) and b-wave (*B*) were recorded by ERG from dark-adapted adequate choline (black circles; $n = 8$) and low choline (red squares; $n = 9$) 2-mo-old mice exposed to low choline diet between E11.5 and E17.5. *C*, *D*) Amplitudes of the a-wave in *A* and b-wave in *B* were recorded by ERG from dark-adapted adequate choline (black circles; $n = 8$) and low choline (red squares; $n = 10$) 2-mo-old mice exposed to low choline diet between E11.5 and P3. $^*P < 0.05$, determined by multiple *t* test (see Supplemental Tables S3 and S4).

factors, such as nutrients, were examined for their possible impact on retinal cytoarchitecture and function [*i.e.*, vitamin A, docosahexaenoic acid (46)]. Here, we report that low availability of choline during pregnancy results in persistent retinal structural defects. Lesions observed in low choline retinas are characterized by the displacement of retinal cells into subretinal space, form predominantly after E17.5 and are consistent with spontaneous, focal disruption of retinal outer limiting membrane (OLM). OLM is created through tight and adherens junctions between the photoreceptor cell inner segments and the end feet of Müller glial cells and is necessary to preserve the integrity of the ONL (47). Abnormal development of retinal Müller glia and rod photoreceptor cells, which arise during mouse postnatal development, was reported to lead to OLM defects (29, 48, 49). In addition, disruption of cell-cell adhesion complexes results in focal disruption of the OLM and consequent displacement and degeneration of photoreceptor cells (50–52). Although in this study we did not directly address differentiation of Müller glia and rod photoreceptors, we found that prolonged exposure to low choline availability, encompassing postnatal development until P3, exacerbates both retinal dysgenesis and function in low choline offspring. In addition, we detected a decrease in Nf2 protein levels in low choline E17.5 retinas. Nf2 is a tumor suppressor, can directly impact the assembly of cell-cell adhesion protein complexes, and regulates contact-dependent cell proliferation (53, 54). Nf2 loss of function mutations lead to optic fissure and neural tube closure defects (55), whereas partial Nf2 loss of function is also sufficient to cause polyneuropathies, retinal hamartomas, epiretinal membranes, and cataracts (56–58). Whether Nf2 expression remains reduced during the postnatal period of retinal development in the offspring exposed to low choline diet *in utero* and can underlie focal disruption of the OLM and occurrence of lesions in low choline retinas remains to be addressed.

Development of photoreceptor cell outer segments, as well as formation of retinal vasculature, also occur postnatally in the mouse retina (59–62). Despite the increase in maternal dietary intake of choline to adequate at E17.5, after a period of low choline diet between E11.5 and E17.5, we find that photoreceptor outer segment ultrastructure in adult low choline offspring remains compromised, whereas retinal blood vessels appear abnormally large. This suggests that despite the restored choline levels in the maternal diet, postnatal development of photoreceptors and retinal vasculature are affected by prenatal low choline availability. In the developing brain, choline was shown to regulate progenitor cell properties through epigenetic mechanisms linked to its role as a methyl-group donor (63–65). Changes in gene expression due to altered DNA and protein methylation, as well as aberrant expression of microRNAs, are examples of the mechanisms that can contribute to long-lasting changes in cell homeostasis due to low choline availability during development. Metabolic imprinting is a term used to characterize the long-term functional consequences of low or high choline availability during brain development (17). Furthermore,

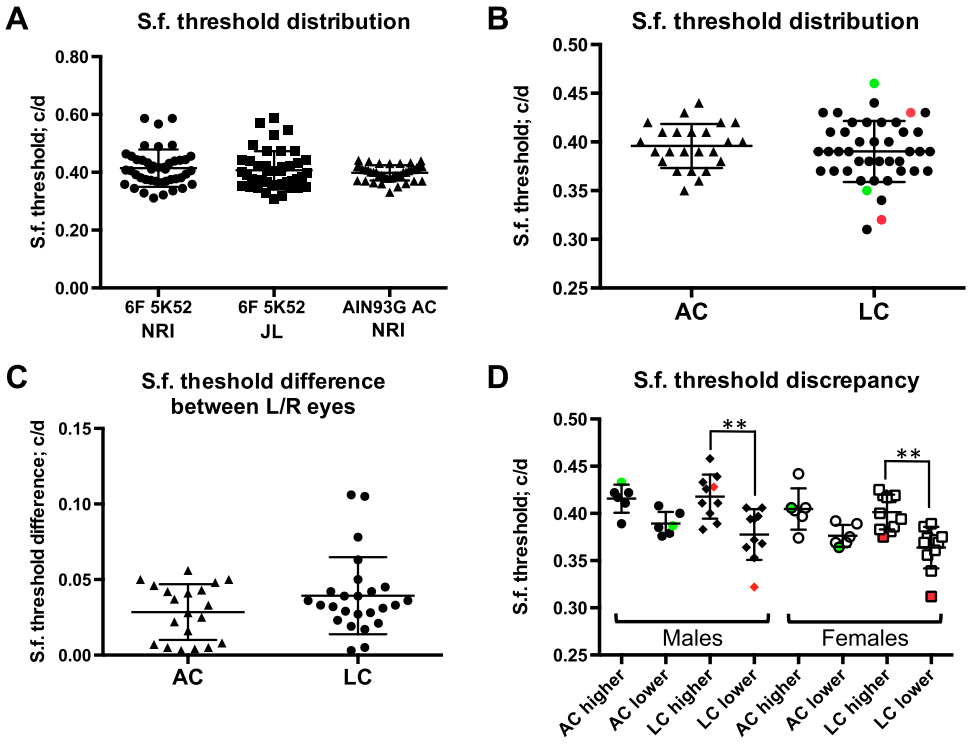


**Figure 8.** Assessment of spatial visual function in adult adequate choline and low choline animals by measuring optokinetic tracking reflex. *A*) Average sf thresholds are not different between animals raised on chow diets at the University of North Carolina Nutrition Research Institute (NRI) or at The Jackson Laboratory, and animals raised on *m*-AIN93G at the NRI. *B*) Analysis of the distribution of the sf thresholds in low choline animals ($n = 13$) reveals a subset of animals with a discrepancy in sf thresholds between the right and the left eyes (green and red data points represent 2 individual animals), compared to adequate choline group ($n = 11$). *C*) Average sf threshold differences between the left and the right eyes are not different between adequate choline and low choline groups. *D*) Average sf thresholds for eyes with higher *vs.* low visual sensitivity are different in low choline males (**$P < 0.01$ by 1-way ANOVA) and in low choline females (**$P < 0.01$ by 1-way ANOVA).

retinal photoreceptor outer segments are composed of tightly packed membrane disks that contain phosphatidylcholine and are renewed throughout life (66, 67). Choline from the extracellular environment is rapidly accumulated in photoreceptor outer segments as phosphatidylcholine, whereas inhibition of this process leads to photoreceptor outer segment degeneration (68, 69). Whether aberrant cone photoreceptor organization and development of retinal vasculature in low choline offspring are driven by persistent epigenetic changes affecting neuronal and endothelial cell types, or by lasting changes in choline metabolism, remains to be elucidated.

In the developing cerebral cortex, low choline availability leads to premature depletion of NPCs through cell cycle exit and differentiation (12, 14). This results in changes in cortical cell type composition and reduced cortical thickness. One of the underlying molecular mechanisms for these effects is up-regulation of a microRNA, miR-129-5p, in NPCs, which inhibits the synthesis of the epidermal growth factor receptor (EGFR) protein (14). EGFR signaling pathway, in turn, is important for the maintenance of NPC self-renewal capacity (14, 70, 71). Here we report that RPC differentiation in low choline retinas is inhibited, possibly explaining hypocellularity observed in a subset of adult low choline retinas. However, EGFR protein expression in the developing mouse retina is not detected until late prenatal/early postnatal stages (72). In this study, we found that increased RPC cell cycle length, combined with maintenance of RPC fate and inhibited neuronal differentiation in low choline embryos, occur during prenatal development, E14.5–E17.5, suggesting that prenatal RPCs employ a different molecular mechanism in response to choline availability.

Reduced Nf2 protein levels observed in low choline embryonic retinas are consistent with inhibition of neuronal differentiation. Nf2 loss of function in RPCs leads to their expansion through persistent cell cycle progression, albeit at a slow rate (73). Importantly, Nf2 function in RPCs is mediated by YAP/TAZ transcriptional coregulators, which in the absence of Nf2 translocate to the nucleus and mediate transcription of multiple target genes (42, 73–75). Consistent with this, loss of YAP function in the retina leads to accelerated RPC cell cycle progression (76), further supporting a hypothesis that increase in YAP/TAZ activity due to partial loss of Nf2 function may explain persistent slow proliferation of low choline RPCs. In this study, we did not detect changes in total YAP/TAZ protein levels between adequate choline and low choline retinas. However, we found that down-regulation of Nf2 is accompanied by the up-regulation of PAK1 (an important regulator of the Hippo signaling pathway), cell cycle progression, and vasculature development (77–79). Detailed analyses of Nf2, YAP/TAZ, and PAK1 phosphorylation status, subcellular localization, and function are necessary to elucidate the links between choline availability and regulation of the Hippo signaling pathway in the retina.

A range of retinal cytoarchitectural defects observed in adult low choline animals suggests that retinal function, and consequently spatial visual sensitivity, may be altered in the offspring exposed to low choline diet during development. Indeed, we found that photoreceptor cell-driven responses, reflected by a-wave amplitudes, are reduced in the offspring exposed to low choline diet prenatally (E11.5–E17.5) or through P3 compared to adequate choline offspring. Interestingly, with shorter exposure to low choline diet (E11.5–E17.5), b-wave amplitudes,

reflecting cumulative responses of the rest of the retinal neurons, are reduced significantly only at low light intensities, suggesting that the input of rod photoreceptors specifically, which are responsible for dim-light and night vision, may not be properly transmitted in low choline retinas. With longer exposure to low choline diet (E11.5-P3), b-wave amplitudes are significantly reduced across light intensities, suggesting that both rod and cone photoreceptor inputs are not translated properly by retinal neurons. Interestingly, we detect that a subset of low choline animals exhibits pronounced discrepancy of nearly 2-fold in a- and b-wave amplitudes between the 2 eyes, suggesting a marked difference in retinal function within the same animals. Reduction in b-wave amplitudes can result from aberrant development of Müller glial cells, which are essential for the maturation of retinal neuronal circuitry (29). Similarly, possible defects in the development of bipolar cells (44, 80), which arise postnatally, can explain a pronounced decrease in b-wave amplitudes in low choline retinas. Addressing how prenatal and postnatal low choline availability impacts the development of retinal circuitry will help corroborate our current findings.

Unlike ERG, optokinetic tracking reflex is influenced by many factors, including the integrity of the circuitry within the visual cortex, and the ability to focus on the image and stabilize head movements (81, 82). Importantly, measurements of visuo-motor behavior using optokinetic tracking system allows for detection of the discrepancies in visual sensitivity between the 2 eyes in the same animal only if the stimulus (grating) is presented within the monocular field of view, with sf thresholds remaining unchanged when the stimulus is presented within the binocular field. In this study, we detected that low choline animals exhibit a discrepancy in visual sensitivity between the left and the right eyes, whereas the average optokinetic motor tracking sf thresholds remained unchanged between the adequate choline and the low choline groups. This suggests a possibility that unequal functional output from individual eyes, driven by retinal cytoarchitectural abnormalities, may underlie activity-dependent establishment of ocular dominance in the visual cortices of low choline animals, causing a condition known as amblyopia (83). Importantly, although affecting 1–5% of all children, amblyopia is more prevalent in developing countries (84), with prenatal and postnatal nutritional status being an important factor in the occurrence of this disorder (85, 86). Although choline status during gestation has not yet been linked to ocular and vision abnormalities in children, none of the systemic health deficits that could potentially result from low choline availability during development and possibly affect vision have been reported.

In humans, development of photoreceptor outer segments and establishment of retinal circuitry are initiated prenatally, with the full complement of retinal cells produced by weeks 19–21 of pregnancy (87). Demand for choline is especially high during pregnancy, whereas the proportion of women obtaining adequate levels of dietary choline intake remains low (1, 88). The results of our study suggest that in the context of genetic and environmental insults leading to retinal disease, low choline availability during pregnancy, manifesting in retinal hypocellularity and a range of cytoarchitectural defects, may exacerbate both the onset and the progression of the disease, as well as contribute to conditions compromising visual perception. Together, our data show that low supply of choline during retinogenesis alters proper temporal progression of neuronal differentiation in the embryonic mouse retina through the regulation of RPC cell cycle exit and cell cycle length dynamics. These findings demonstrate, for the first time, that in addition to its requirement for brain development, adequate supply of choline is also necessary for the development of the visual system. FJ

## ACKNOWLEDGMENTS

The authors thank Dr. David Horita [Nutrition Research Institute, University of North Carolina (UNC)–Chapel Hill, Kannapolis, NC, USA] for critically evaluating this manuscript; Ms. Lorian Molina-Torres (Nutrition Research Institute, UNC–Chapel Hill) for help with data acquisition and analyses; The Microscopy Services Laboratory, Department of Pathology and Laboratory Medicine at the UNC–Chapel Hill (Chapel Hill, NC, USA), especially Mrs. Victoria Madden (UNC–Chapel Hill), for transmission electron microscopy sample preparation and imaging. This work was supported by U.S. National Institutes of Health (NIH), National Institute of Diabetes and Digestive and Kidney Diseases Grants DK056350 and DK115380 (to S.H.Z.). The Microscopy Services Laboratory, Department of Pathology and Laboratory Medicine, is supported in part by P30 CA016086 Cancer Center Core Support Grant to the UNC–Chapel Hill Lineberger Comprehensive Cancer Center. Listed funding sources were not involved in the progress and outcomes of this study or in publication decision. The corresponding authors had full access to all the data reported in this study and had final responsibility to submit this work for publication. The authors declare no conflicts of interest.

## AUTHOR CONTRIBUTIONS

I. Trujillo-Gonzalez conducted experiments, collected the data, analyzed the data, and wrote the manuscript; W. B. Friday and C. A. Munson conducted experiments, collected the data, and analyzed the data; A. Bachleda conducted experiments, collected the data, and analyzed the data; E. R. Weiss designed the experiments and analyzed the data; N. M. Alam conducted experiments and analyzed the data; W. Sha analyzed the data; S. H. Zeisel designed the study and wrote the manuscript; N. Surzenko designed the study, conducted experiments, collected the data, analyzed the data, prepared the figures, and wrote the manuscript.

## REFERENCES

1. Zeisel, S. H. (2006) Choline: critical role during fetal development and dietary requirements in adults. *Annu. Rev. Nutr.* **26**, 229–250
2. Tayebati, S. K., Marucci, G., Santinelli, C., Buccioni, M., and Amenta, F. (2015) Choline-containing phospholipids: structure-activity relationships versus therapeutic applications. *Curr. Med. Chem.* **22**, 4328–4340
3. Amenta, F., and Tayebati, S. K. (2008) Pathways of acetylcholine synthesis, transport and release as targets for treatment of adult-onset cognitive dysfunction. *Curr. Med. Chem.* **15**, 488–498
4. Zeisel, S. (2017) Choline, other methyl-donors and epigenetics. *Nutrients* **9**, E445

5. Boeke, C. E., Gillman, M. W., Hughes, M. D., Rifas-Shiman, S. L., Villamor, E., and Oken, E. (2013) Choline intake during pregnancy and child cognition at age 7 years. *Am. J. Epidemiol.* **177**, 1338–1347
6. Wallace, T. C., McBurney, M., and Fulgoni V. L. III (2014) Multivitamin/mineral supplement contribution to micronutrient intakes in the United States, 2007-2010. *J. Am. Coll. Nutr.* **33**, 94–102
7. Dominguez-Salas, P., Moore, S. E., Cole, D., da Costa, K. A., Cox, S. E., Dyer, R. A., Fulford, A. J., Innis, S. M., Waterland, R. A., Zeisel, S. H., Prentice, A. M., and Hennig, B. J. (2013) DNA methylation potential: dietary intake and blood concentrations of one-carbon metabolites and cofactors in rural African women. *Am. J. Clin. Nutr.* **97**, 1217–1227
8. Shaw, G. M., Carmichael, S. L., Laurent, C., and Rasmussen, S. A. (2006) Maternal nutrient intakes and risk of orofacial clefts. *Epidemiology* **17**, 285–291
9. Gossell-Williams, M., Fletcher, H., McFarlane-Anderson, N., Jacob, A., Patel, J., and Zeisel, S. (2005) Dietary intake of choline and plasma choline concentrations in pregnant women in Jamaica. *West Indian Med. J.* **54**, 355–359
10. Fischer, L. M., daCosta, K. A., Kwock, L., Stewart, P. W., Lu, T. S., Stabler, S. P., Allen, R. H., and Zeisel, S. H. (2007) Sex and menopausal status influence human dietary requirements for the nutrient choline. *Am. J. Clin. Nutr.* **85**, 1275–1285
11. Resseguie, M. E., da Costa, K. A., Galanko, J. A., Patel, M., Davis, I. J., and Zeisel, S. H. (2011) Aberrant estrogen regulation of PEMT results in choline deficiency-associated liver dysfunction. *J. Biol. Chem.* **286**, 1649–1658
12. Wang, Y., Surzenko, N., Friday, W. B., and Zeisel, S. H. (2016) Maternal dietary intake of choline in mice regulates development of the cerebral cortex in the offspring. *FASEB J.* **30**, 1566–1578
13. Craciunescu, C. N., Albright, C. D., Mar, M. H., Song, J., and Zeisel, S. H. (2003) Choline availability during embryonic development alters progenitor cell mitosis in developing mouse hippocampus. *J. Nutr.* **133**, 3614–3618
14. Trujillo-Gonzalez, I., Wang, Y., Friday, W. B., Vickers, K. C., Toth, C. L., Molina-Torres, L., Surzenko, N., and Zeisel, S. H. (2019) MicroRNA-129-5p is regulated by choline availability and controls EGF receptor synthesis and neurogenesis in the cerebral cortex. *FASEB J.* **33**, 3601–3612
15. Meck, W. H., and Williams, C. L. (1997) Perinatal choline supplementation increases the threshold for chunking in spatial memory. *Neuroreport* **8**, 3053–3059
16. Meck, W. H., Smith, R. A., and Williams, C. L. (1988) Pre- and postnatal choline supplementation produces long-term facilitation of spatial memory. *Dev. Psychobiol.* **21**, 339–353
17. Meck, W. H., and Williams, C. L. (2003) Metabolic imprinting of choline by its availability during gestation: implications for memory and attentional processing across the lifespan. *Neurosci. Biobehav. Rev.* **27**, 385–399
18. Meck, W. H., Williams, C. L., Cermak, J. M., and Blusztajn, J. K. (2008) Developmental periods of choline sensitivity provide an ontogenetic mechanism for regulating memory capacity and age-related dementia. *Front. Integr. Nuerosci.* **1**, 7
19. Caudill, M. A., Strupp, B. J., Muscalu, L., Nevins, J. E. H., and Canfield, R. L. (2018) Maternal choline supplementation during the third trimester of pregnancy improves infant information processing speed: a randomized, double-blind, controlled feeding study. *FASEB J.* **32**, 2172–2180
20. Fuhrmann, S. (2010) Eye morphogenesis and patterning of the optic vesicle. *Curr. Top. Dev. Biol.* **93**, 61–84
21. Cook, T. (2003) Cell diversity in the retina: more than meets the eye. *BioEssays* **25**, 921–925
22. Javed, A., and Cayouette, M. (2017) Temporal progression of retinal progenitor cell identity: implications in cell replacement therapies. *Front. Neural Circuits* **11**, 105
23. Cepko, C. L. (1999) The roles of intrinsic and extrinsic cues and bHLH genes in the determination of retinal cell fates. *Curr. Opin. Neurobiol.* **9**, 37–46
24. Mattar, P., and Cayouette, M. (2015) Mechanisms of temporal identity regulation in mouse retinal progenitor cells. *Neurogenesis (Austin)* **2**, e1125409
25. Encinas, J. M., Vaahtokari, A., and Enikolopov, G. (2006) Fluoxetine targets early progenitor cells in the adult brain. *Proc. Natl. Acad. Sci. USA* **103**, 8233–8238
26. Lagace, D. C., Whitman, M. C., Noonan, M. A., Ables, J. L., DeCarolis, N. A., Arguello, A. A., Donovan, M. H., Fischer, S. J., Farnbauch, L. A., Beech, R. D., DiLeone, R. J., Greer, C. A., Mandyam, C. D., and Eisch, A. J. (2007) Dynamic contribution of nestin-expressing stem cells to adult neurogenesis. *J. Neurosci.* **27**, 12623–12629
27. Madisen, L., Zwingman, T. A., Sunkin, S. M., Oh, S. W., Zariwala, H. A., Gu, H., Ng, L. L., Palmiter, R. D., Hawrylycz, M. J., Jones, A. R., Lein, E. S., and Zeng, H. (2010) A robust and high-throughput Cre reporting and characterization system for the whole mouse brain. *Nat. Neurosci.* **13**, 133–140
28. Phillips, M. J., Walker, T. A., Choi, H. Y., Faulkner, A. E., Kim, M. K., Sidney, S. S., Boyd, A. P., Nickerson, J. M., Boatright, J. H., and Pardue, M. T. (2008) Tauroursodeoxycholic acid preservation of photoreceptor structure and function in the rd10 mouse through postnatal day 30. *Invest. Ophthalmol. Vis. Sci.* **49**, 2148–2155
29. Bachleda, A. R., Pevny, L. H., and Weiss, E. R. (2016) Sox2-deficient müller glia disrupt the structural and functional maturation of the mammalian retina. *Invest. Ophthalmol. Vis. Sci.* **57**, 1488–1499
30. Liang, K. J., Woodard, K. T., Weaver, M. A., Gaylor, J. P., Weiss, E. R., and Samulski, R. J. (2017) AAV-Nrf2 promotes protection and recovery in animal models of oxidative stress. *Mol. Ther.* **25**, 765–779
31. Prusky, G. T., Alam, N. M., Beekman, S., and Douglas, R. M. (2004) Rapid quantification of adult and developing mouse spatial vision using a virtual optomotor system. *Invest. Ophthalmol. Vis. Sci.* **45**, 4611–4616
32. Douglas, R. M., Alam, N. M., Silver, B. D., McGill, T. J., Tschetter, W. W., and Prusky, G. T. (2005) Independent visual threshold measurements in the two eyes of freely moving rats and mice using a virtual-reality optokinetic system. *Vis. Neurosci.* **22**, 677–684
33. Heavner, W. E., Andoniadou, C. L., and Pevny, L. H. (2014) Establishment of the neurogenic boundary of the mouse retina requires cooperation of SOX2 and WNT signaling. *Neural Dev.* **9**, 27
34. Martynoga, B., Morrison, H., Price, D. J., and Mason, J. O. (2005) Foxg1 is required for specification of ventral telencephalon and region-specific regulation of dorsal telencephalic precursor proliferation and apoptosis. *Dev. Biol.* **283**, 113–127
35. Benjamini, Y., and Hochberg, Y. (1995) Controlling the false discovery rate: a practical and powerful approach to multiple testing. Journal of the Royal Statistical Society Series B *(Methodological)* **57**, 289–300
36. Kolb, H. (1995) Photoreceptors. In *Webvision: The Organization of the Retina and Visual System* (Kolb, H., Fernandez, E., and and Nelson, R., eds.), pp. 1–12, University of Utah Health Sciences Center, Salt Lake City, UT, USA
37. Kolb, H. (1995) Cone pathways through the retina. In *Webvision: The Organization of the Retina and Visual System* (Kolb, H., Fernandez, E., and and Nelson, R., eds.), pp. 98–155, University of Utah Health Sciences Center, Salt Lake City, UT, USA
38. Hafler, B. P., Surzenko, N., Beier, K. T., Punzo, C., Trimarchi, J. M., Kong, J. H., and Cepko, C. L. (2012) Transcription factor Olig2 defines subpopulations of retinal progenitor cells biased toward specific cell fates. *Proc. Natl. Acad. Sci. USA* **109**, 7882–7887
39. Fields-Berry, S. C., Halliday, A. L., and Cepko, C. L. (1992) A recombinant retrovirus encoding alkaline phosphatase confirms clonal boundary assignment in lineage analysis of murine retina. *Proc. Natl. Acad. Sci. USA* **89**, 693–697
40. Baye, L. M., and Link, B. A. (2008) Nuclear migration during retinal development. *Brain Res.* **1192**, 29–36
41. Zhao, B., Li, L., Lei, Q., and Guan, K. L. (2010) The Hippo-YAP pathway in organ size control and tumorigenesis: an updated version. *Genes Dev.* **24**, 862–874
42. Lee, M., Goraya, N., Kim, S., and Cho, S. H. (2018) Hippo-yap signaling in ocular development and disease. *Dev. Dyn.* **247**, 794–806
43. Robson, J. G., and Frishman, L. J. (2014) The rod-driven a-wave of the dark-adapted mammalian electroretinogram. *Prog. Retin. Eye Res.* **39**, 1–22
44. McCall, M. A., and Gregg, R. G. (2008) Comparisons of structural and functional abnormalities in mouse b-wave mutants. *J. Physiol.* **586**, 4385–4392
45. Marquardt, T. (2003) Transcriptional control of neuronal diversification in the retina. *Prog. Retin. Eye Res.* **22**, 567–577
46. Lien, E. L., and Hammond, B. R. (2011) Nutritional influences on visual development and function. *Prog. Retin. Eye Res.* **30**, 188–203
47. Omri, S., Omri, B., Savoldelli, M., Jonet, L., Thillaye-Goldenberg, B., Thuret, G., Gain, P., Jeanny, J. C., Crisanti, P., and Behar-Cohen, F. (2010) The outer limiting membrane (OLM) revisited: clinical implications. *Clin. Ophthalmol.* **4**, 183–195

48. Surzenko, N., Crowl, T., Bachleda, A., Langer, L., and Pevny, L. (2013) SOX2 maintains the quiescent progenitor cell state of postnatal retinal Muller glia. *Development* **140**, 1445–1456
49. Campbell, M., Humphries, M., Kenna, P., Humphries, P., and Brankin, B. (2007) Altered expression and interaction of adherens junction proteins in the developing OLM of the Rho(-/-) mouse. *Exp. Eye Res.* **85**, 714–720
50. Gosens, I., den Hollander, A. I., Cremers, F. P., and Roepman, R. (2008) Composition and function of the Crumbs protein complex in the mammalian retina. *Exp. Eye Res.* **86**, 713–726
51. Mehalow, A. K., Kameya, S., Smith, R. S., Hawes, N. L., Denegre, J. M., Young, J. A., Bechtold, L., Haider, N. B., Tepass, U., Heckenlively, J. R., Chang, B., Naggert, J. K., and Nishina, P. M. (2003) CRB1 is essential for external limiting membrane integrity and photoreceptor morphogenesis in the mammalian retina. *Hum. Mol. Genet.* **12**, 2179–2189
52. Mattapallil, M. J., Wawrousek, E. F., Chan, C. C., Zhao, H., Roychoudhury, J., Ferguson, T. A., and Caspi, R. R. (2012) The Rd8 mutation of the Crb1 gene is present in vendor lines of C57BL/6N mice and embryonic stem cells, and confounds ocular induced mutant phenotypes. *Invest. Ophthalmol. Vis. Sci.* **53**, 2921–2927
53. Cooper, J., and Giancotti, F. G. (2014) Molecular insights into NF2/Merlin tumor suppressor function. *FEBS Lett.* **588**, 2743–2752
54. Curto, M., and McClatchey, A. I. (2008) Nf2/Merlin: a coordinator of receptor signalling and intercellular contact. *Br. J. Cancer* **98**, 256–262
55. McLaughlin, M. E., Kruger, G. M., Slocum, K. L., Crowley, D., Michaud, N. A., Huang, J., Magendantz, M., and Jacks, T. (2007) The Nf2 tumor suppressor regulates cell-cell adhesion during tissue fusion. *Proc. Natl. Acad. Sci. USA* **104**, 3261–3266
56. Schulz, A., Baader, S. L., Niwa-Kawakita, M., Jung, M. J., Bauer, R., Garcia, C., Zoch, A., Schacke, S., Hagel, C., Mautner, V. F., Hanemann, C. O., Dun, X. P., Parkinson, D. B., Weis, J., Schröder, J. M., Gutmann, D. H., Giovannini, M., and Morrison, H. (2013) Merlin isoform 2 in neurofibromatosis type 2-associated polyneuropathy. *Nat. Neurosci.* **16**, 426–433
57. Asthagiri, A. R., Parry, D. M., Butman, J. A., Kim, H. J., Tsilou, E. T., Zhuang, Z., and Lonser, R. R. (2009) Neurofibromatosis type 2. *Lancet* **373**, 1974–1986
58. Hanemann, C. O., Diebold, R., and Kaufmann, D. (2007) Role of NF2 haploinsufficiency in NF2-associated polyneuropathy. *Brain Pathol.* **17**, 371–376
59. Swaroop, A., Kim, D., and Forrest, D. (2010) Transcriptional regulation of photoreceptor development and homeostasis in the mammalian retina. *Nat. Rev. Neurosci.* **11**, 563–576
60. Wheway, G., Parry, D. A., and Johnson, C. A. (2014) The role of primary cilia in the development and disease of the retina. *Organogenesis* **10**, 69–85
61. Ramamurthy, V., and Cayouette, M. (2009) Development and disease of the photoreceptor cilium. *Clin. Genet.* **76**, 137–145
62. Selvam, S., Kumar, T., and Fruttiger, M. (2018) Retinal vasculature development in health and disease. *Prog. Retin. Eye Res.* **63**, 1–19
63. Mehedint, M. G., Niculescu, M. D., Craciunescu, C. N., and Zeisel, S. H. (2010) Choline deficiency alters global histone methylation and epigenetic marking at the Re1 site of the calbindin 1 gene. *FASEB J.* **24**, 184–195
64. Niculescu, M. D., Craciunescu, C. N., and Zeisel, S. H. (2006) Dietary choline deficiency alters global and gene-specific DNA methylation in the developing hippocampus of mouse fetal brains. *FASEB J.* **20**, 43–49
65. Blusztajn, J. K., and Mellott, T. J. (2012) Choline nutrition programs brain development via DNA and histone methylation. *Cent. Nerv. Syst. Agents Med. Chem.* **12**, 82–94
66. Zemski Berry, K. A., Gordon, W. C., Murphy, R. C., and Bazan, N. G. (2014) Spatial organization of lipids in the human retina and optic nerve by MALDI imaging mass spectrometry. *J. Lipid Res.* **55**, 504–515
67. Goldberg, A. F., Moritz, O. L., and Williams, D. S. (2016) Molecular basis for photoreceptor outer segment architecture. *Prog. Retin. Eye Res.* **55**, 52–81
68. Masland, R. H., and Mills, J. W. (1980) Choline accumulation by photoreceptor cells of the rabbit retina. *Proc. Natl. Acad. Sci. USA* **77**, 1671–1675
69. Pu, G. A., and Anderson, R. E. (1983) Alteration of retinal choline metabolism in an experimental model for photoreceptor cell degeneration. *Invest. Ophthalmol. Vis. Sci.* **24**, 288–293
70. Burrows, R. C., Wancio, D., Levitt, P., and Lillien, L. (1997) Response diversity and the timing of progenitor cell maturation are regulated by developmental changes in EGFR expression in the cortex. *Neuron* **19**, 251–267
71. Sun, Y., Goderie, S. K., and Temple, S. (2005) Asymmetric distribution of EGFR receptor during mitosis generates diverse CNS progenitor cells. *Neuron* **45**, 873–886
72. Lillien, L., and Wancio, D. (1998) Changes in epidermal growth factor receptor expression and competence to generate glia regulate timing and choice of differentiation in the retina. *Mol. Cell. Neurosci.* **10**, 296–308
73. Moon, K. H., Kim, H. T., Lee, D., Rao, M. B., Levine, E. M., Lim, D. S., and Kim, J. W. (2018) Differential expression of NF2 in neuroepithelial compartments is necessary for mammalian eye development. *Dev. Cell.* **44**, 13–28.e3
74. Cao, X., Pfaff, S. L., and Gage, F. H. (2008) YAP regulates neural progenitor cell number via the TEA domain transcription factor. *Genes Dev.* **22**, 3320–3334
75. Lavado, A., He, Y., Paré, J., Neale, G., Olson, E. N., Giovannini, M., and Cao, X. (2013) Tumor suppressor Nf2 limits expansion of the neural progenitor pool by inhibiting Yap/Taz transcriptional coactivators. *Development* **140**, 3323–3334
76. Cabochette, P., Vega-Lopez, G., Bitard, J., Parain, K., Chemouny, R., Masson, C., Borday, C., Hedderich, M., Henningfeld, K. A., Locker, M., Bronchain, O., and Perron, M. (2015) YAP controls retinal stem cell DNA replication timing and genomic stability. *Elife* **4**, e08488
77. Kissil, J. L., Wilker, E. W., Johnson, K. C., Eckman, M. S., Yaffe, M. B., and Jacks, T. (2003) Merlin, the product of the Nf2 tumor suppressor gene, is an inhibitor of the p21-activated kinase, Pak1. *Mol. Cell* **12**, 841–849
78. Pan, X., Chang, X., Leung, C., Zhou, Z., Cao, F., Xie, W., and Jia, Z. (2015) PAK1 regulates cortical development via promoting neuronal migration and progenitor cell proliferation. *Mol. Brain* **8**, 36
79. Kelly, M. L., Astsaturov, A., and Chernoff, J. (2013) Role of p21-activated kinases in cardiovascular development and function. *Cell. Mol. Life Sci.* **70**, 4223–4228
80. Suzuki-Kerr, H., Iwagawa, T., Sagara, H., Mizota, A., Suzuki, Y., and Watanabe, S. (2018) Pivotal roles of Fezf2 in differentiation of cone OFF bipolar cells and functional maturation of cone ON bipolar cells in retina. *Exp. Eye Res.* **171**, 142–154
81. Prusky, G. T., Alam, N. M., and Douglas, R. M. (2006) Enhancement of vision by monocular deprivation in adult mice. *J. Neurosci.* **26**, 11554–11561
82. Cahill, H., and Nathans, J. (2008) The optokinetic reflex as a tool for quantitative analyses of nervous system function in mice: application to genetic and drug-induced variation. *PLoS One* **3**, e2055
83. Bonaccorsi, J., Berardi, N., and Sale, A. (2014) Treatment of amblyopia in the adult: insights from a new rodent model of visual perceptual learning. *Front. Neural Circuits* **8**, 82
84. Gilbert, C. E., and Ellwein, L. B.; Refractive Error Study in Children Study Group. (2008) Prevalence and causes of functional low vision in school-age children: results from standardized population surveys in Asia, Africa, and Latin America. *Invest. Ophthalmol. Vis. Sci.* **49**, 877–881
85. Gyawali, R., Bhayal, B. K., Adhikary, R., Shrestha, A., and Sah, R. P. (2017) Retrospective data on causes of childhood vision impairment in Eritrea. *BMC Ophthalmol.* **17**, 209
86. Brémond-Gignac, D., Copin, H., Lapillonne, A., and Milazzo, S.; European Network of Study and Research in Eye Development. (2011) Visual development in infants: physiological and pathological mechanisms. *Curr. Opin. Ophthalmol.* **22** (Suppl), S1–S8
87. Finlay, B. L. (2008) The developing and evolving retina: using time to organize form. *Brain Res.* **1192**, 5–16
88. Wallace, T. C., and Fulgoni V. L. III (2016) Assessment of total choline intakes in the United States. *J. Am. Coll. Nutr.* **35**, 108–112


*Received for publication February 15, 2019.*
*Accepted for publication April 15, 2019.*